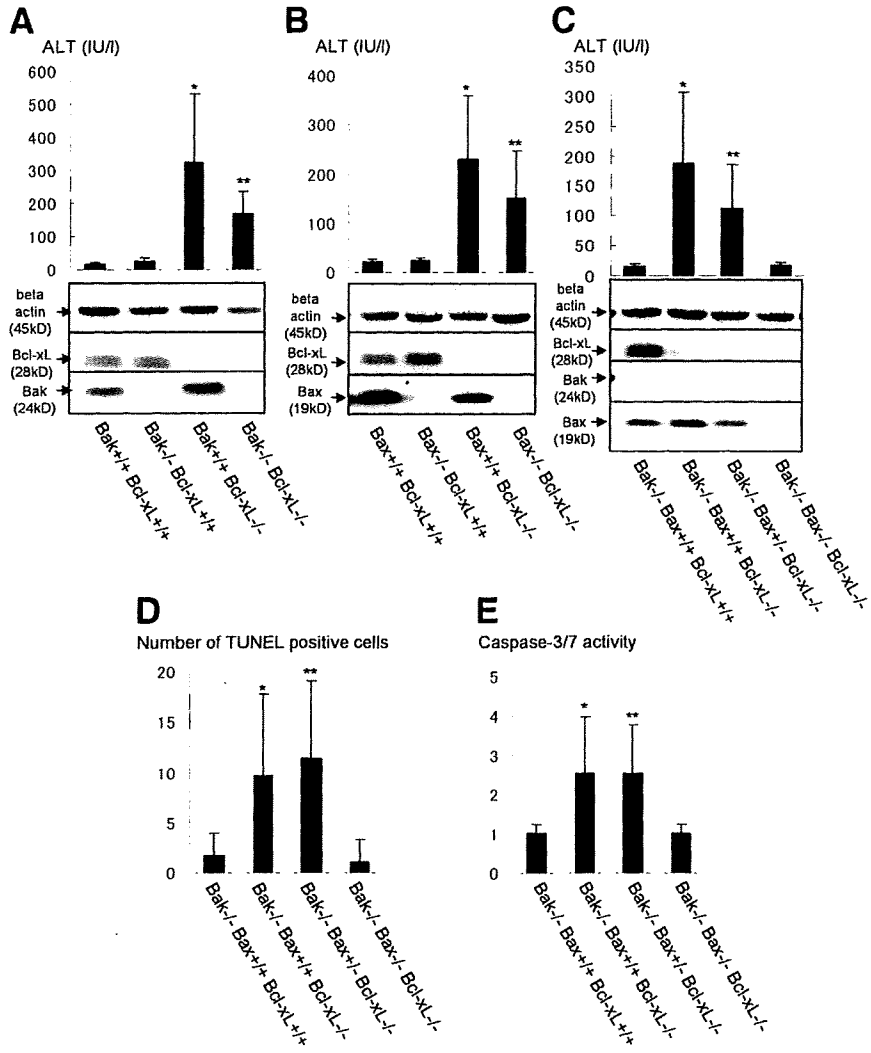


Fig. 2. Bcl-xL KO mice with Bak or Bax KO background. (A) Offspring from mating *bak*$^{+/-}$ *bcl-x*$^{flox/flox}$ *AlbCre* mice and *bak*$^{+/-}$ *bcl-x*$^{flox/flox}$ mice were sacrificed at 6 weeks after birth. Serum ALT levels and western blot of whole liver lysate for the expression of Bcl-xL and Bak are shown. N = 14 mice per group. * and **$P < 0.05$ versus the other three groups. (B) Offspring from mating *bax*$^{+/-}$ *bcl-x*$^{flox/flox}$ *AlbCre* mice and *bax*$^{+/-}$ *bcl-x*$^{flox/flox}$ mice were sacrificed at 6 weeks after birth. Serum ALT levels and western blot of whole liver lysate for the expression of Bcl-xL and Bax are shown. N = 15 mice per group. * and **$P < 0.05$ versus the other two Bcl-xL+/+ groups. (C, D, and E) Offspring from mating *bak*$^{-/-}$ *bax*$^{flox/+}$ *bcl-x*$^{flox/flox}$ *AlbCre* mice and *bak*$^{-/-}$ *bax*$^{flox/+}$ *bcl-x*$^{flox/flox}$ mice were sacrificed at 6 weeks after birth. Bax+/+ stands for *bax*$^{flox/flox}$ without *AlbCre*, and Bax−/− stands for *bax*$^{flox/flox}$ with *AlbCre*. N = 8 or 10 mice per group. Serum ALT levels and western blot of whole liver lysate for the expression of Bcl-xL, Bak, and Bax are shown (C). *$P < 0.05$ versus Bak−/− Bax+/+ Bcl-xL+/+ and Bak−/− Bax−/− Bcl-xL−/− groups; **$P < 0.05$ versus Bak−/− Bax−/− Bcl-xL−/− group. Statistics of TUNEL-positive cells (D). * and **$P < 0.05$ versus Bak−/− Bax+/+ Bcl-xL+/+ and Bak−/− Bax−/− Bcl-xL−/− groups. Serum caspase-3/7 activity (E). * and **$P < 0.05$ versus Bak−/− Bax+/+ Bcl-xL+/+ and Bak−/− Bax−/− Bcl-xL−/− groups.

mice, there was no difference between two groups in serum ALT levels (Supporting Fig. 3A), caspase-3/7 activity (Supporting Fig. 3B), and the ratios of liver weight to body weight (Supporting Fig. 3C), which suggests that healthy hepatocytes in wild-type mice are completely protected from Bid or Bak/Bax-mediated apoptosis by Bcl-xL.

***Bcl-xL Interacts with Cytosolic Bax and Mitochondrial Bak in the Liver.*** To examine the expression of a variety of Bcl-2–related molecules in the liver, cytosolic and mitochondrial fractions from liver lysate were subjected to western blot analysis (Fig. 3A). Anti-apoptotic Bcl-2 proteins, Bcl-xL and Mcl-1, were expressed at both the mitochondria and the cytosol. In contrast, Bak and Bax were exclusively expressed at the mitochondria and the cytosol, respectively. Full-length Bid was expressed mainly in the cytosol. To examine whether Bcl-xL physically interacts with those Bcl-2–related proteins, liver lysate was immunoprecipitated with Bcl-xL and identified using corresponding antibodies (Fig. 3B). At least a part of Bcl-xL was bound to Bak and Bax, but not to Mcl-1 or full-length Bid.

***tBid, But Not Full-Length Bid, Displaces Bak and Bax from Bcl-xL by Binding to Bcl-xL.*** Bcl-2–like molecules have been shown to be capable of binding Bak or Bax, and through this interaction, to neutralize each activity.[17] Conversely, other research showed that Bcl-xL does not have to bind Bax-like molecules to protect against cell death.[18] To examine the impact of tBid on the association between Bcl-xL and Bak or Bax, we added tBid to the liver lysate and examined the interaction of each Bcl-2–related protein with Bcl-xL by immunoprecipitation. Addition of 500 nM tBid abolished the association between Bcl-xL and Bak or Bax (Supporting Fig. 4). Simultaneously, Bcl-xL binding of tBid was observed. Addition of 20 nM tBid also abolished, if not completely, the association between Bcl-xL and Bak or Bax (Fig. 4). In contrast, adding the same concentration of full-length Bid had little effect on Bcl-xL binding of Bak or Bax (Fig. 4). These results indicated that tBid can bind to Bcl-xL

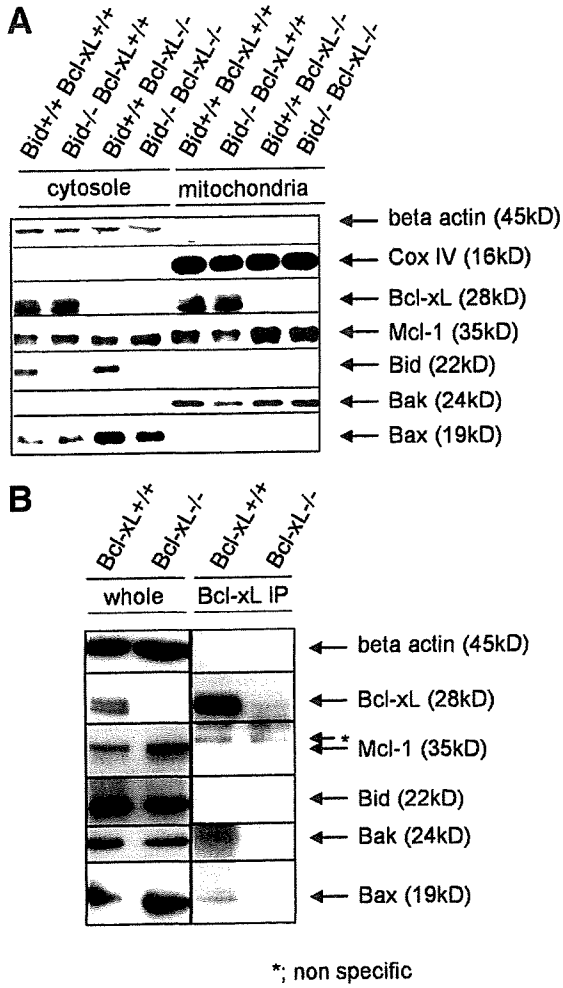


Fig. 3. Expression of Bcl-2-related molecules in the liver and their association with Bcl-xL. Bcl-xL+/+ stands for *bcl-x*$^{flox/flox}$ without *AlbCre*, and Bcl-xL−/− stands for *bcl-x*$^{flox/flox}$ with *AlbCre*. (A) Western blot after cellular fractionations of the liver lysate. Loading amounts of cytosolic and mitochondrial fractions were adjusted to be equivalent for the starting liver samples. (B) Western blot after anti-Bcl-xL immunoprecipitation. Whole cellular lysate and immunoprecipitates with anti-Bcl-xL were verified with the indicated antibodies. Samples from Bcl-xL−/− mice were included as a negative control.

and suggest that tBid binding of Bcl-xL unleashes Bak or Bax from Bcl-xL.

***A Small But Significant Level of tBid Is Detected in the Healthy Liver.*** Genetic evidence that Bid is required for Bak/Bax-dependent apoptosis caused by Bcl-xL deficiency and biochemical evidence that full-length Bid is inactive for displacing Bak or Bax from Bcl-xL together suggest that tBid is produced in wild-type liver. To confirm this, we performed western blot analysis using antibody that can detect tBid (Fig. 5A). Liver lysate from Bid KO mice served as a negative control, whereas that from wild-type mice injected with anti-Fas antibody served as a positive control. A significant level of tBid was detected in wild-type liver, although the amount was smaller than in Fas-stimulated mice, which displayed massive live cell apoptosis.

***Bcl-xL–Deficient Mitochondria Are Susceptible to a Trace Amount of tBid.*** To examine the impact of a small amount of tBid on Bcl-xL–deficient mitochondria, tBid or full-length Bid at various concentrations was incubated with mitochondria isolated from Bcl-xL–deficient liver or wild-type liver (Fig. 5B). In agreement with previous reports,[19] wild-type mitochondria efficiently released cytochrome c on exposure to tBid. Full-length Bid was far less effective at releasing cytochrome c. Importantly, Bcl-xL–deficient mitochondria were capable of releasing cytochrome c on exposure to a smaller amount of tBid than wild-type mitochondria. This agrees with the in vivo findings that Bcl-xL–deficient hepatocytes, but not wild-type hepatocytes, underwent apoptosis with a trace amount of tBid.

***Administration of ABT-737 Produces ALT Elevation in Wild-Type Mice But to a Lesser Extent in Bid KO Mice.*** Bcl-2–like molecules have been receiving attention as a target for inducing apoptosis, especially in cancer cells.[20] A variety of BH3 mimetics that interact with the hydrophobic groove of anti-apoptotic Bcl-2 proteins has been developed. They inhibit binding of anti-apoptotic Bcl-2–like molecules with BH3-only proteins and presumably with Bak and Bax. ABT-737, a prototype of this class of agents, was designed to mimic the BH3-only protein Bad and can inhibit the function of Bcl-2, Bcl-xL, or Bcl-w but not that of Mcl-1.[21] Our data on Bcl-xL KO mice raised the possibility that pharmacological inhibition of Bcl-xL may cause hepatocyte apoptosis. To examine this possibility, we injected ABT-737 and examined the liver injury. As expected, the levels of ALT

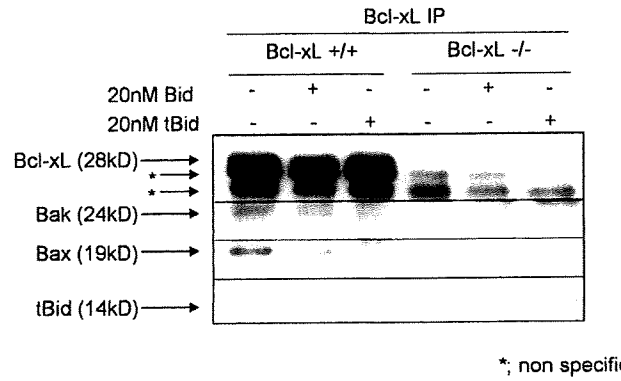


Fig. 4. tBid binds to Bcl-xL and displaces Bak or Bax from Bcl-xL. Liver lysate from *bcl-x*$^{flox/flox}$ without *AlbCre* (Bcl-xL+/+) and *bcl-x*$^{flox/flox}$ with *AlbCre* (Bcl-xL−/−) were incubated with or without 20 nM recombinant tBid or recombinant full-length Bid at 37°C for 20 minutes. After immunoprecipitation with Bcl-xL, immunoprecipitates are verified with indicated antibodies. Immunoprecipitated lysate from Bcl-xL−/− mice was loaded as a negative control.

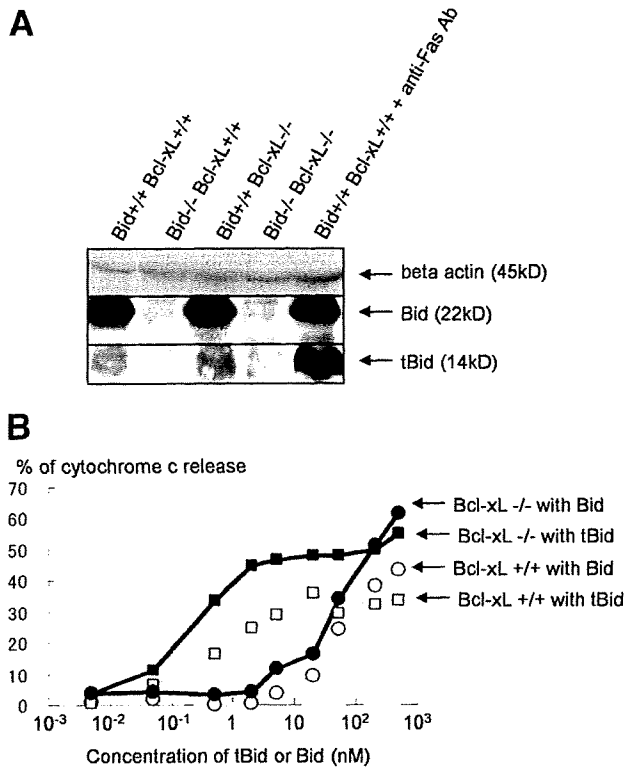


Fig. 5. A small amount of tBid is expressed in wild-type liver and is sufficient for producing cytochrome c release from Bcl-xL-deficient mitochondria. (A) Western blot of liver lysate for Bid and tBid expression. Lysate from wild-type (Bid+/+ Bcl-xL+/+) mice 1 hour after intravenous injection of 10 $\mu$g anti-Fas antibody (clone Jo2) and from Bid−/− mice were included as a positive and a negative control of tBid, respectively. (B) Mitochondrial release of cytochrome c to tBid. Mitochondria were isolated from Bcl-xL-deficient or wild-type liver and incubated with recombinant tBid or recombinant full-length Bid at various concentrations for 30 minutes. Similar results were obtained in three times repeated experiments.

were clearly elevated in wild-type mice (Fig. 6A). TUNEL staining of the liver section showed apoptosis in hepatocytes scattered in the liver lobule (Fig. 6B). Importantly, no significant elevation of serum ALT levels was observed with a Bak/Bax double-KO background. The data indicated that genetic and pharmacological ablation of Bcl-xL led to a similar apoptosis phenotype in the liver.

To examine the impact of Bid in ABT-737–induced hepatocyte apoptosis, ABT-737 was administered to wild-type mice and Bid KO mice. Elevation of serum ALT levels was ameliorated with a Bid KO background (Fig. 6C). It has been well established that administration of ABT-737 led to acute thrombocytopenia.[22] This was explained by the fact that Bcl-xL is a critical apoptosis antagonist in platelets.[10] In our experiment, the counts of circulating platelets declined significantly in the wild-type mice (Fig. 6D), which is in the agreement with previous studies.[10] Interestingly, a similar degree of thrombocytopenia was observed even in Bid KO mice, suggesting that Bid does not play a significant role in regulating platelet homeostasis, unlike in hepatocytes. The data imply that the impact of Bid in the Bcl-2 network in healthy cells is cell-type specific.

## Discussion

One of the important findings of the current study is that the BH3-only protein Bid is an essential molecule for apoptosis of differentiated hepatocytes caused by Bcl-xL deficiency. This is surprising, because differentiated hepatocytes are generally considered to be quiescent cells. Organ homeostasis may be ensured in two ways: one is through turnover of cells, and the other is by the quies-

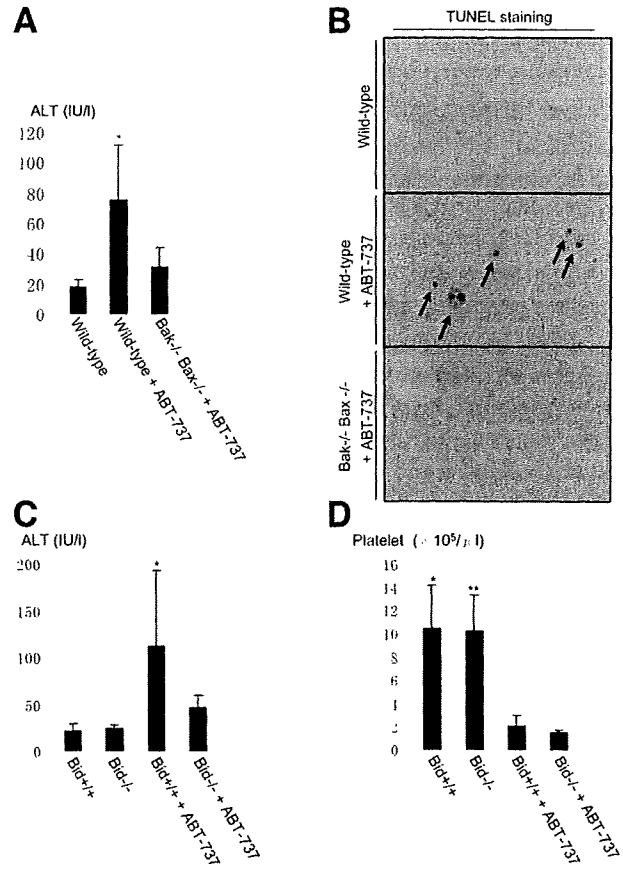


Fig. 6. ABT-737 administration in wild-type, Bak/Bax double-KO, and Bid KO mice. (A and B) Wild-type mice or hepatocyte-specific Bak/Bax double-KO mice were challenged with intraperitoneal injection of ABT-737 at 100 mg/kg or vehicle alone and sacrificed 16 hours later. Serum ALT levels (A) and representative pictures of TUNEL staining in the liver (B) are shown. N = 5 or more than 5 mice per group. *$P < 0.05$ versus the other two groups. (C and D) Wild-type mice or Bid KO mice were challenged with intraperitoneal injection of ABT-737 at 100 mg/kg or vehicle alone and sacrificed 16 hours later. Serum ALT levels (C) and circulating platelet counts (D) were determined. N = 5 or more than 5 mice per group. *$P < 0.05$ versus the other three groups for (C); * and **$P < 0.05$ versus the other two groups, with ABT-737 for (D).

cence of matured cells. Typical examples for the former are hematopoietic organs, intestine and skin, whereas those for the latter are a variety of solid organs, such as the liver, lung, pancreas, heart, and brain. Because hematopoietic cells die at particular time points to maintain host homeostasis, it would not be surprising that their life span may be controlled by a variety of death signals. Indeed, Bim KO mice have excess hematopoietic cells, particularly lymphocytes, suggesting that Bim strictly controls homeostasis of hematopoietic cells.[23] In contrast, healthy cells in the solid organs are usually considered to not suffer from apoptotic stimuli. Although interaction between core Bcl-2 proteins and BH3-only proteins is important for understanding apoptosis regulation, little work has been done by generating mice simultaneously deficient in molecules of both groups. To the best of our knowledge, the only example clearly using this approach is a study on Bim/Bcl-2 double-KO mice that showed that growth retardation, skin abnormality, and lymphoid cell reduction found in Bcl-2 KO mice were ameliorated with a Bim-deficient background.[24] This suggested that lymphoid cells constitutively sense Bim-mediated killing signals, and, without Bcl-2, decrease in number. The current study is the first demonstration that parenchymal cells in a solid organ such as differentiated hepatocytes also suffer from Bid-mediated BH3 stress.

Bid is ubiquitously expressed in many cell types. Generally, Bid is inactive for death induction and is activated on proteolytic cleavage by caspase-8 or other proteases. In the current study, we found that not only full-length Bid but also tBid could be detected in wild-type liver. Administration of tBid, but not that of full-length Bid, at 20 nM in wild-type liver lysate or mitochondria was sufficient for unleashing Bak or Bax from Bcl-xL and releasing cytochrome c. Conversely, a lesser amount of tBid (for example, at 2 nM) was sufficient for inducing cytochrome c release from Bcl-xL–deficient mitochondria. These results are consistent with the idea that a small amount of tBid produced in the liver could activate cytochrome c release and apoptosis in hepatocytes of the Bcl-xL–deficient mice. What mechanisms are involved in the production of tBid from full-length Bid in the healthy liver is not known yet. Our results suggest that Myd88 and TNF-$\alpha$ may not be involved in the activation of tBid under physiological conditions. However, other ligation of death receptors such as Fas, and TNF-related apoptosis-inducing ligand receptor, can cause caspase-8 activation followed by Bid cleavage.[15,25] Bile salts, which are consistently produced in and secreted from hepatocytes, are capable of inducing hepatocyte apoptosis through Fas activation.[26] Natural killer cells are predominant lymphocytes accumulating in the liver and constitutively express TNF-related apoptosis-inducing ligand.[27] Further study is needed to examine what kinds of stresses activate the Bid pathway in a physiological setting.

Adult differentiated hepatocytes express at least two anti-apoptotic Bcl-2 proteins, Bcl-xL and Mcl-1, but not prototype Bcl-2.[8] Recently, Vick et al.[28] reported that hepatocyte-specific Mcl-1 KO mice developed naturally occurring apoptosis in hepatocytes. We also independently generated hepatocyte-specific Mcl-1 KO mice and obtained an apoptosis phenotype that could not be distinguished from that of hepatocyte-specific Bcl-xL KO mice.[29] Thus, Mcl-1, like Bcl-xL, plays a critical role in maintaining integrity of differentiated hepatocytes. There are two major models regarding how BH3-only proteins mediate Bak/Bax-dependent apoptosis: a direct model and an indirect model.[30] From the viewpoint of the indirect model, our data would mean a small amount of tBid is sequestered by Bcl-xL and Mcl-1 and, without Bcl-xL, is sufficient for neutralizing Mcl-1 to promote apoptosis. Conversely, from the viewpoint of the direct model, both Bcl-xL and Mcl-1 are needed to completely sequester a small amount of tBid, and without Bcl-xL, unleashed tBid would directly activate Bak and Bax. In the current study, we observed that tBid when administered in liver lysate could bind to Bcl-xL. This observation seems to agree with the indirect model, although we could not exclude the possibility of the direct model. Further study will be needed by developing Bid/Bcl-xL/Mcl-1 KO mice to examine the underlying mechanisms of how activated Bid regulates the mitochondrial pathway of apoptosis in the liver.

Malignant tumors frequently overexpress one or more members of the anti-apoptotic Bcl-2 family, which confers the resistance of tumor cells to apoptosis.[31,32] Recently, small molecules targeting specific anti-apoptotic Bcl-2 family proteins have been developed for treatment of cancer therapy.[33,34] The underlying concept of this strategy is the difference in addiction to anti-apoptotic Bcl-2 family proteins between normal cells and transformed cells. In general, normal cells are not considered to suffer from apoptotic stimuli or to have activated BH3-only proteins. In contrast, transformed cells suffer from a variety of apoptotic stimuli such as genotoxic *p53* activation and environmental stresses, and possess activated BH3-only molecules. If a single anti-apoptotic Bcl-2 protein is neutralized by a small molecule, it could release BH3-only molecules, which then neutralize other anti-apoptotic Bcl-2 proteins or directly activate Bax-like molecules, leading to cell death. However, the current study clearly indicated that normal hepatocytes could be under activation of Bid, raising concern that hepatocyte injury may be produced if Bcl-xL function is completely knocked down. Indeed, we have shown that administra-

tion of a high dose of ABT-737, which is an antagonist for Bcl-xL/Bcl-2, not for Mcl-1,[21] induced Bak/Bax-dependent hepatocyte apoptosis in wild-type mice but to a lesser extent in Bid KO mice. Therefore, special caution should be paid to hepatotoxicity when systemically administering a high dose of Bcl-xL–targeting molecules, because hepatocytes are suffering from Bid-mediated stresses.

In conclusion, we have demonstrated here that the BH3-only protein Bid is activated and antagonized by anti-apoptotic Bcl-2 family proteins under physiological conditions. BH3 stress or Bcl-2 addiction is not a unique characteristic of tumor cells. Even in healthy cells, cellular integrity is not controlled by a simple rheostat between Bax-like molecules and Bcl-2–like molecules. The current study reveals a previously unrecognized complicated network of Bcl-2 family proteins controlling the integrity of healthy cells. Dissection of the Bcl-2 network will be important for further understanding of liver pathophysiology.

*Acknowledgment:* The authors thank Abbott Laboratories for providing ABT-737.

## References


1. Youle RJ, Strasser A. The BCL-2 protein family: opposing activities that mediate cell death. Nat Rev Mol Cell Biol 2008;9:47-59.
2. Korsmeyer SJ, Shutter JR, Veis DJ, Merry DE, Oltvai ZN. Bcl-2/Bax: a rheostat that regulates an anti-oxidant pathway and cell death. Semin Cancer Biol 1993;4:327-332.
3. Puthalakath H, Strasser A. Keeping killers on a tight leash: transcriptional and post-translational control of the pro-apoptotic activity of BH3-only proteins. Cell Death Differ 2002;9:505-512.
4. Willis SN, Adams JM. Life in the balance: how BH3- only proteins induce apoptosis. Curr Opin Cell Biol 2005;17:617-625.
5. Yin XM. Bid, a BH3-only multi-functional molecule, is at the cross road of life and death. Gene 2006;369:7-19.
6. Scaffidi C, Fulda S, Srinivasan A, Friesen C, Li F, Tomaselli KJ, et al. Two CD95 (APO-1/Fas) signaling pathways. EMBO J 1998;17:1675-1687.
7. Yin XM, Wang K, Gross A, Zhao Y, Zinkel S, Klocke B, et al. Bid-deficient mice are resistant to Fas-induced hepatocellular apoptosis. Nature 1999; 400:886-891.
8. Takehara T, Tatsumi T, Suzuki T, Rucker EB III, Hennighausen L, Jinushi M, et al. Hepatocyte-specific disruption of Bcl-xL leads to continuous hepatocyte apoptosis and liver fibrotic responses. Gastroenterology 2004;127:1189-1197.
9. Shindler KS, Latham CB, Roth KA. Bax deficiency prevents the increased cell death of immature neurons in bcl-x-deficient mice. J Neurosci 1997; 17:3112-3119.
10. Mason KD, Carpinelli MR, Fletcher JI, Collonge JE, Hilton AA, Ellis S, et al. Programmed anuclear cell death delimits platelet life span. Cell 2007; 128:1173-1186.
11. Wagner KU, Claudio E, Rucker EB 3rd, Riedlinger G, Broussard C, Schwartzberg PL, et al. Conditional deletion of the Bcl-x gene from erythroid cells results in hemolytic anemia and profound splenomegaly. Development 2000;127:4949-4958.
12. Takeuchi O, Fisher J, Suh H, Harada H, Malynn BA, Korsmeyer SJ. Essential role of BAX,BAK in B cell homeostasis and prevention of autoimmune disease. Proc Natl Acad Sci U S A 2005;102:11272-11277.
13. Takehara T, Hayashi N, Tatsumi T, Kanto T, Mita E, Sasaki Y, et al. Interleukin 1beta protects mice from Fas-mediated hepatocyte apoptosis and death. Gastroenterology 1999;117:661-668.
14. Wang K, Yin XM, Chao DT, Milliman CL, Korsmeyer SJ. BID: a novel BH3 domain-only death agonist. Genes Dev 1996;10:2859-2869.
15. Luo X, Budihardjo I, Zou H, Slaughter C, Wang X. Bid, a Bcl2 interacting protein, mediates cytochrome c release from mitochondria in response to activation of cell surface death receptors. Cell 1998;94:481-490.
16. Seki E, Brenner DA. Toll-like receptors and adaptor molecules in liver disease: update. HEPATOLOGY 2008;48:322-335.
17. Willis SN, Chen L, Dewson G, Wei A, Naik E, Fletcher JI, et al. Proapoptotic Bak is sequestered by Mcl-1 and Bcl-xL, but not Bcl-2, until displaced by BH3-only proteins. Genes Dev 2005;19:1129-1305.
18. Liu X, Zhu Y, Dai S, White J, Peyerl F, Kappler JW, et al. Bcl-xl does not have to bind Bax to protect T cells from death. J Exp Med 2006;203:2953-2961.
19. Kim TH, Zhao Y, Barber MJ, Kuharsky DK, Yin XM. Bid-induced cytochrome c release is mediated by a pathway independent of mitochondrial permeability transition pore and Bax. J Biol Chem 2000;275:39474-39481.
20. Adams JM, Cory S. Bcl-2-regulated apoptosis: mechanism and therapeutic potential. Curr Opin Immunol 2007;19:488-496.
21. Oltersdorf T, Elmore SW, Shoemaker AR, Armstrong RC, Augeri DJ, Belli BA, et al. An inhibitor of Bcl-2 family proteins induces regression of solid tumours. Nature 2005;435:677-681.
22. Zhang H, Nimmer PM, Tahir SK, Chen J, Fryer RM, Hahn KR, et al. Bcl-2 family proteins are essential for platelet survival. Cell Death Differ 2007;14:943-951.
23. Bouillet P, Metcalf D, Huang DCS, Tarlinton DM, Kay TWH, Köntgen F, et al. Proapoptotic Bcl-2 relative Bim required for certain apoptotic responses, leukocyte homeostasis, and to preclude autoimmunity. Science 1999;286:1735-1738.
24. Bouillet P, Cory S, Zhang LC, Strasser A, Adams JM. Degenerative disorders caused by Bcl-2 deficiency prevented by loss of its BH3-only antagonist Bim. Dev Cell 2001;1:645-653.
25. Yamada H, Tada-Oikawa S, Uchida A, Kawanishi S. TRAIL causes cleavage of bid by caspase-8 and loss of mitochondrial membrane potential resulting in apoptosis in BJAB cells. Biochem Biophys Res Commun 1999; 265:130-133.
26. Faubion WA, Guicciardi ME, Miyoshi H, Bronk SF, Roberts PJ, Svingen PA, et al. Toxic bile salts induce rodent hepatocyte apoptosis via direct activation of Fas. J Clin Invest 1999;103:137-145.
27. Takeda K, Hayakawa Y, Smyth MJ, Kayagaki N, Yamaguchi N, Kakuta S, et al. Involvement of tumor necrosis factor-related apoptosis-inducing ligand in surveillance of tumor metastasis by liver natural killer cells. Nat Med 2001;7:94-100.
28. Vick B, Weber A, Urbanik T, Maass T, Teufel A, Krammer PH, et al. Knockout of myeloid cell leukemia-1 induces liver damage and increases apoptosis susceptibility of murine hepatocytes. HEPATOLOGY 2009;49:627-636.
29. Hikita H, Takehara T, Shimizu S, Kodama T, Li W, Miyagi T, et al. Mcl-1 and Bcl-xL cooperatively maintain integrity of hepatocytes in developing and adult murine liver. HEPATOLOGY 2009; doi:10.1002/hep.23126.
30. Chipuk JE, Green DR. How do BCL-2 proteins induce mitochondrial outer membrane permeabilization? Trends Cell Biol 2008;18:157-164.
31. Takehara T, Liu X, Fujimoto J, Friedman SL, Takahashi H. Expression and role of Bcl-xL in human hepatocellular carcinomas. HEPATOLOGY 2001;34:55-61.
32. Takehara T, Takahashi H. Suppression of Bcl-xL deamidation in human hepatocellular carcinomas. Cancer Res 2003;63:3054-3057.
33. Labi V, Grespi F, Baumgartner F, Villunger A. Targeting the Bcl-2-regulated apoptosis pathway by BH3 mimetics: a breakthrough in anticancer therapy? Cell Death Differ 2008;15:977-987.
34. Mott JL, Gores GJ. Piercing the armor of hepatobiliary cancer: Bcl-2 homology domain 3 (BH3) mimetics and cell death. HEPATOLOGY 2007; 46:906-911.

Cancer Immunol Immunother (2010) 59:453–463
DOI 10.1007/s00262-009-0764-x

ORIGINAL ARTICLE

# Natural killer cell is a major producer of interferon γ that is critical for the IL-12-induced anti-tumor effect in mice

**Akio Uemura · Tetsuo Takehara · Takuya Miyagi · Takahiro Suzuki · Tomohide Tatsumi · Kazuyoshi Ohkawa · Tatsuya Kanto · Naoki Hiramatsu · Norio Hayashi**

Received: 12 February 2009 / Accepted: 24 August 2009 / Published online: 16 September 2009


**Abstract** Although the anti-tumor effect of IL-12 is mediated mostly by IFNγ, which cell types most efficiently produce IFNγ and therefore initiate or promote the anti-tumor effect of IL-12 has not been clearly determined. In the present study, we demonstrated hydrodynamic injection of the IL-12 gene led to prolonged IFNγ production, NK-cell activation and complete inhibition of liver metastasis of CT-26 colon cancer cells in wild-type mice, but not in IFNγ knockout mice. NK cells expressed higher levels of STAT4 and upon IL-12 administration displayed stronger STAT4 phosphorylation and IFNγ production than non-NK cells. Adoptive transfer of wild-type NK cells into IFNγ knockout mice restored IL-12-induced IFNγ production, NK-cell activation and anti-tumor effect, whereas transfer of the same number of wild-type non-NK cells did not. In conclusion, NK cells are predominant producers of IFNγ that is critical for IL-12 anti-tumor therapy.

**Keywords** IFNγ · Innate immunity · Liver tumor · IL-12 · NK

A. Uemura and T. Takehara contributed equally to this work.

**Electronic supplementary material** The online version of this article (doi:10.1007/s00262-009-0764-x) contains supplementary material, which is available to authorized users.

A. Uemura · T. Takehara · T. Miyagi · T. Suzuki · T. Tatsumi · K. Ohkawa · T. Kanto · N. Hiramatsu · N. Hayashi (✉)
Department of Gastroenterology and Hepatology,
Osaka University Graduate School of Medicine,
2-2 Yamada-oka, Suita, Osaka 565-0871, Japan
e-mail: hayashin@gh.med.osaka-u.ac.jp

A. Uemura
e-mail: akioue@gh.med.osaka-u.ac.jp

## Introduction

IL-12 is a 70-kDa heterodimer protein, composed of p35 and p40 subunits, mainly produced by antigen-presenting cells. IL-12 was originally found as a "natural killer-stimulating factor" and a "cytotoxic lymphocyte maturation factor" [1, 2]. IL-12 has multi-potent effects, inducing a Th1 response, enhancing the CD8 T-cell response, activating natural killer cells and inducing production of IFNγ [3, 4]. Therapeutic use of IL-12, either using its recombinant protein or gene, can induce an efficient anti-tumor effect on primary or metastatic tumors in various murine models and humans [5, 6].

Research has shown that IL-12 mediates anti-tumor effects in a variety of ways. They include anti-proliferative effects, anti-angiogenic effects [7, 8] and cytotoxic effects of effector lymphocytes. A variety of effector cells has been reported to be required for IL-12-mediated anti-tumor effects: they include CD8 T cells [9], NKT cells [10], CD4 T cells [11] and NK cells [12]. The relative contribution of these cells may differ among IL-12 doses and types of tumor models [13]. Endogenous IFNγ production is required for most, if not all, of the anti-tumor effects of IL-12 administration [14, 15]. IL-12 stimulates a variety of immune cells, such as T cells [16], B cells [17] and NK cells [18], to produce IFNγ. However, which cell types are most critical for producing IFNγ during IL-12 therapy is not clearly known.

In the present study, we used a murine model of liver metastasis of CT-26 colon cancer cells and found that NK cells highly expressed the IL-12 signaling molecule STAT4 and most efficiently produced IFNγ. IFNγ was essential for the anti-tumor effect of IL-12, and NK-cell production of IFNγ sufficed to produce the full-blown anti-tumor effects. These results demonstrated that NK cells

serve not only as an effector but also as an important mediator producing IFNγ that is critical for the anti-tumor effects of IL-12.

## Materials and methods

### Mice

Specific pathogen-free female Balb/c mice were purchased from Clea Japan, Inc (Tokyo, Japan). Rag2 knockout (Rag2 KO) mice with a Balb/c background were purchased from Taconic (Germantown, NY). IFNγ knockout (GKO) mice with a Balb/c background were kindly provided by Dr. Yoichiro Iwakura (Institute of Medical Science, University of Tokyo). All mice used were at the age of 6 to 10 weeks. They were housed under conditions of controlled temperature and light with free access to food and water at the Institute of Experimental Animal Science, Osaka University Graduate School of Medicine. All animals received humane care, and the study protocol complied with the institution's guidelines.

### Tumor models

Intra-splenic injection of tumor cells was used to establish micro-disseminated liver tumors in mice [19]. CT-26 colon cancer cells originating from Balb/c mice were maintained in RPMI1620 supplemented with 10% FCS. Syngeneic mice were anesthetized with pentobarbital and given a cut on the left side flank. CT-26 cells ($1 \times 10^5$) were suspended in 200 μl of PBS and injected into the spleen.

### Injection of naked plasmid DNA

A plasmid coding the murine IL-12 gene, pCMV-IL-12, was generously provided by Dr. M Watanabe (Laboratory of Experimental Immunology, Division of Basic Sciences, National Cancer Institute-Frederick Cancer Research and Development Center) [20]. Plasmid DNA was prepared using an EndoFree plasmid system (Qiagen, Hilden, Germany,) according to the manufacturer's instructions. Hydrodynamic injection of plasmid DNA was performed as previously described [21]. In brief, 25 μg of plasmid DNA was diluted with 2.0 ml of lactated Ringer's solution and injected into the tail vein, using a syringe with a 26-gauge needle. DNA injection was completed within 5 to 8 s.

### ELISA

Blood samples were serially obtained from the venous plexus in the retro-orbita under light anesthesia. The levels of serum IL-12 p70, IFNγ (BD Biosciences-Pharmingen, San Diego, CA), IFNγ-inducible protein 10 (IP-10) and monokine induced by IFNγ (MIG) (R&D Systems, Inc, Minneapolis, MN) were measured using commercially available ELISA kits in accordance with the manufacturer's instructions.

### Mononuclear cells

Mononuclear cells were isolated from the liver or spleen as previously described. The NK activity of mononuclear cells was assessed by a standard 4-h $^{51}$Cr-releasing assay using Yac1 cells as targets. In some experiments, mononuclear cells were separated into $DX5^+$ cells (NK cells) and $DX5^-$ cells (non-NK cells) using the MACS system (Miltenyi Biotec GmbH, Bergisch Gladbach, Germany). The purity of the isolated NK-cell population was found to be greater than 90% by FACS analysis.

### Flow cytometric analysis

Liver mononuclear cells were isolated 2 days after pCMV-IL-12 injection. Cytokine secretion was then blocked by the addition of brefeldin A for 4 h. Next, liver mononuclear cells were stained with FITC-conjugated anti-TCRβ antibody and biotin-conjugated anti-CD49b antibody (DX5), fixed and permeabilized with Cytofix/Cytoperm (BD Biosciences), and stained with PE-conjugated anti-INFγ antibody or corresponding isotype controls. Analysis was performed using a FACSCalibur (Becton Dickinson), with the resulting data analyzed using the CELLQuest program (Becton Dickinson). NK cells were identified as $DX5^+/TCR\beta^-$ lymphocytes, NKT cells as $DX5^+/TCR\beta^+$ lymphocytes and T cells as $DX5^-/TCR\beta^+$ lymphocytes.

### Adoptive transfer

For adoptive transfer experiments, GKO mice were injected intravenously 1 day before plasmid DNA injection with $2.0 \times 10^8$ whole mononuclear cells or $4.0 \times 10^6$ NK cells, or non-NK cells or whole mononuclear cells, all of which had been harvested from wild-type mice that can produce IFNγ.

### Western blotting

Mouse recombinant IL-12 was purchased from R&D Systems, Inc (Minneapolis, MN). Mononuclear cells were treated with or without IL-12. Whole cell lysate was prepared from mononuclear cells from mice, and 20 μg of protein was separated by SDS-PAGE and transferred to the PVDF membrane. The membrane was stained with anti-STAT4 antibody (BD biosciences),

anti-phospho-specific STAT4 (pY693) antibody (BD biosciences), anti-STAT1 antibody (Cell Signaling), anti-phospho-specific STAT1 antibody (Cell Signaling) and visualized by chemiluminescence.

### NK-cell depletion

For depletion of NK cells in vivo, anti-asialoGM1 antibody (WAKO, Osaka, Japan) was intraperitoneally administered. We determined the appropriate dosing to be 500 μg/mouse (50 μl when dissolved according to the manufacturer's instructions) based on FACS analysis of hepatic mononuclear cells. The percentage of $DX5^+/TCR\beta^-$ cells (NK cells) is 12.6 ± 2.4% in IgG-injected liver, whereas it decreased to 0.76 ± 0.04% one day after anti-asialo GM1 antibody injection ($N = 3$/group). This effect remained at least 3 days after anti-asialo GM1 antibody injection. NKT cells were less affected than NK cells, because 90% of $DX5^+/TCR\beta^+$ cells (NKT cells) still remained in the liver after the treatment. Anti-asialoGM1 antibody was injected 1 day after tumor inoculation and then every 5 days. For the control, the same amount of normal rabbit immunoglobulin (DAKO, Copenhagen, Denmark) was intraperitoneally administered.

### Histology

The formalin-fixed livers were paraffin-embedded, and liver sections were analyzed by hematoxylin-eosin staining. Acetone-fixed fresh frozen liver sections were immunostained with anti-mouse CD4 (H123.19), anti-mouse CD8α (53-6.7) or anti-CD31 (390) monoclonal antibody (all from BD Biosciences), using a VECSTAIN ABC kit (Vector Laboratories, Burlingame, California, USA).

### Statistics

Data are represented as mean ± SD. Comparisons between groups were analyzed by unpaired $t$-test with Welch's correction. $p < 0.05$ was considered statistically significant.

## Results

### Hydrodynamic injection of IL-12-expressing plasmid led to prolonged production of IFNγ

Hydrodynamics-based gene delivery into mice establishes efficient foreign gene expression predominantly in the liver, especially in hepatocytes. Serial measurement of serum IL-12 demonstrated that pCMV-IL-12 injection led to substantial IL-12 production on day 1. The levels of serum IL-12 then rapidly declined (Fig. 1a). We also measured IFNγ production in serum, since IL-12 is known to activate IFNγ production. pCMV-IL-12 and, to a lesser extent, pCMV injection increased serum IFNγ on day 1. In contrast to the pCMV injection group, high levels of serum IFNγ were maintained at later time points in the pCMV-IL-12 injection group (Fig. 1a). Thus, hydrodynamic injection of pCMV-IL-12 led to prolonged production of IFNγ. Transient IFNγ production followed by control plasmid may be an indirect effect of liver injury caused by bolus injection of saline or DNA injection.

### IL-12 therapy induced NK activation and anti-metastatic effects, both of which are critically dependent on IFNγ

To examine the biological effects of the produced IL-12, we evaluated the NK activity of mononuclear cells from the liver. pCMV-IL-12 injection, but not control pCMV injection, increased Yac1 lytic activity of hepatic mononuclear cells (Fig. 1b). When GKO mice were injected with pCMV-IL-12 or pCMV, the hepatic mononuclear cells did not display any lytic ability to Yac1 cells, suggesting that IL-12-mediated NK-cell activation required IFNγ.

To examine the anti-metastatic effect of IL-12, pCMV-IL-12 or pCMV was injected into wild-type mice 2 days after intrasplenic injection of CT-26 cells. At 14 days after tumor injection, the mice were killed for evaluation of liver tumor (Fig. 1c). While pCMV-injected mice displayed huge liver tumors, pCMV-IL-12-injected mice did not show any macroscopic or microscopic tumor (Fig. 1d). Liver weight was significantly higher in pCMV-injected mice than pCMV-IL-12-injected mice, reflecting liver tumor formation. To examine the involvement of IFNγ in the IL-12-induced anti-tumor effect, we injected pCMV or pCMV-IL-12 into GKO mice 2 days after CT-26 injection. At 14 days after CT-26 injection, both groups showed similar degrees of tumor formation and there was no significant difference in liver weight between the two. This indicated that IL-12-induced anti-metastatic effect was strictly dependent on IFNγ.

### NK cells were the most potent producer of IFNγ during IL-12 therapy

To evaluate which cell types most efficiently produced IFNγ, we isolated hepatic mononuclear cells from mice 2 days after plasmid injection and then stained cell surface TCRβ and DX5 as well as intracellular IFNγ (Fig. 2). $TCR\beta^-/DX5^+$ NK cells, $TCR\beta^+/DX5^+$ NKT cells and $TCR\beta^+/DX5^-$ T cells from pCMV-IL-12-injected mice showed significant levels of IFNγ production compared

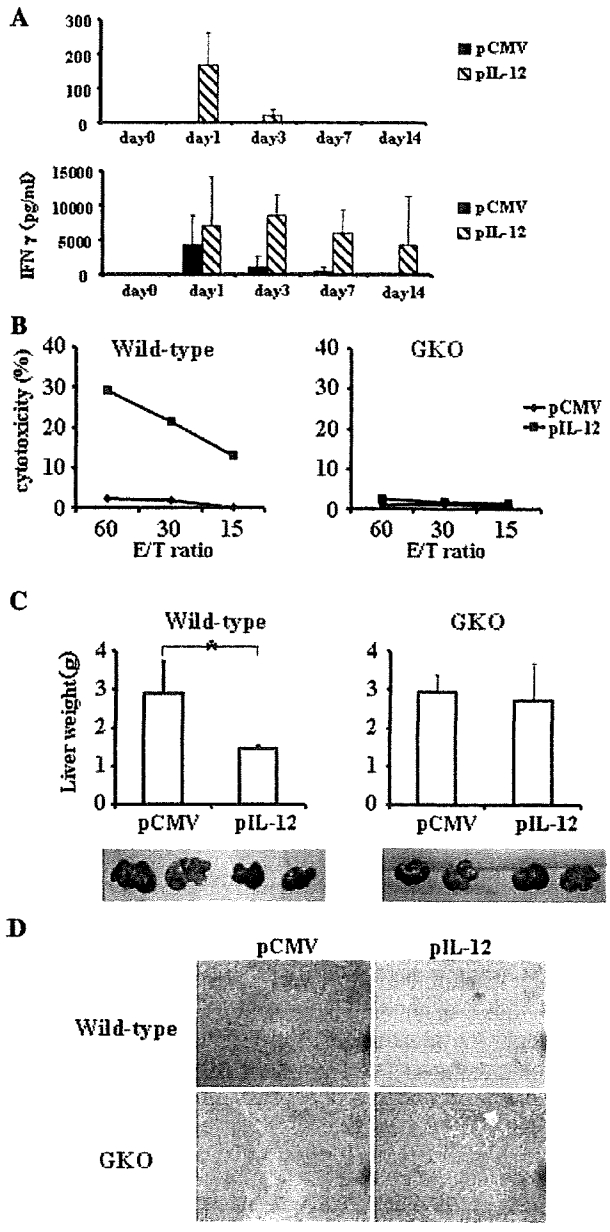


**Fig. 1** Effects of hydrodynamic injection of IL-12-encoding plasmid. **a** Wild-type mice were hydrodynamically injected with either pCMV-IL-12 (*hatched bars*) or pCMV (*closed bars*) and bled at the indicated time points to measure the levels of serum IL-12 and IFNγ. Results are indicated as mean and SD ($n = 6$/group). **b** NK-cell activation after IL-12 administration. Hepatic mononuclear cells were isolated from wild-type mice (*left*) or GKO mice (*right*) which had been injected with pCMV-IL-12 (*closed squares*) or pCMV (*closed diamonds*) 4 days earlier. Yac1 lytic ability was measured by a standard $^{51}$Cr-release assay at the indicated effector and target ratios (E/T ratio). All experiments were performed at least 3 times and representative data are shown. **c** and **d** Anti-metastatic effects of IL-12 therapy. Wild-type mice (*left*) or GKO mice (*right*) were intrasplenically injected with CT-26 cells and, 2 days later, hydrodynamically injected with either pCMV-IL-12 or pCMV. At 14 days after the plasmid injection, the mice were killed to examine liver tumor development. **c** Data are indicated as mean and SD of the liver weight at the top ($n = 6$/group) and a representative picture of the liver in each group is shown at the bottom. *$p < 0.001$. **d** Representative histology of liver sections

with those from naive mice or pCMV-injected mice. The levels of IFNγ production were highest in NK cells among those cells. Even at a later time point, 7 days after plasmid injection, NK cells were found to produce the highest levels of IFNγ (data not shown).

## IL-12-induced STAT4 signaling and IFNγ production increased in NK cells

IL-12 activates Janus kinases Tyk2 and Jak2, STAT4 as well as other STATs. To examine the activation of STAT1 and STAT4, we isolated splenocytes from wild-type mice and GKO mice and stimulated them with IL-12 and/or IFNγ in the presence or absence of anti-IFNγ Ab (Fig. 3a). IL-12 led to phosphorylation of both STAT1 and STAT4 in wild-type splenocytes. In contrast, the same treatment led to phosphorylation of STAT4, but not of STAT1, in GKO splenocytes. Addition of IFNγ restored STAT1 phosphorylation in GKO splenocytes. Furthermore, adding anti-IFNγ inhibited STAT1 phosphorylation in wild-type cells. These findings demonstrated that phosphorylation of STAT4 is a direct effect of IL-12 but phosphorylation of STAT1 is indirect, via an autocrine or paracrine IFNγ-dependent manner.

To examine STAT1 and STAT4 activation and IFNγ production in NK cells and non-NK cells, we prepared whole mononuclear cells as well as NK and non-NK populations from wild-type spleens and stimulated the cells with IL-12 (Fig. 3b). NK cells expressed higher levels of STAT4 than non-NK cells. Upon IL-12 treatment, STAT4 was rapidly phosphorylated in NK cells, but to a lesser extent in non-NK cells. In contrast, NK cells expressed lesser levels of STAT1 than non-NK cells. STAT1 was similarly phosphorylated in NK cells and non-NK cells upon IL-12 treatment. Both NK cells and non-NK cells produced significant levels of IFNγ, but the levels were much higher in NK cells than non-NK cells (Fig. 3c). These results indicated that compared with non-NK cells, NK cells possessed higher levels of STAT4, a direct signaling molecule of IL-12, and produced higher levels of IFNγ than non-NK cells.

## NK cells were sufficient for IL-12-mediated anti-tumor effects

The above observation indicated that NK cells are a predominant producer of IFNγ, which was critical for the IL-12-induced anti-tumor effects. To examine whether NK

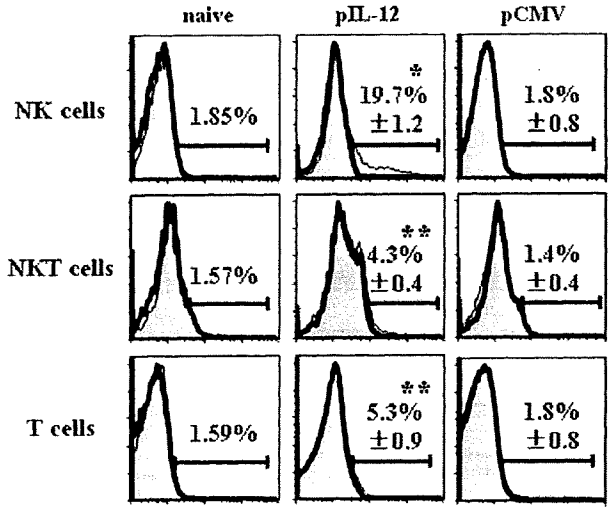


**Fig. 2** IFNγ expression of mononuclear cells after IL-12 administration. Wild-type mice were injected with pCMV-IL-12 or pCMV, or were untreated (naive). Mononuclear cells were isolated from the liver 2 days after plasmid injection and stained with anti-TCRβ mAb, anti-DX5 mAb and anti-IFNγ mAb. *Closed histograms* show the IFNγ expression in the gated populations ($TCR\beta^+/DX5^+$ cells for NK cells, $TCR\beta^+/DX5^+$ cells for NKT cells and $TCR\beta^+/DX5^-$ cells for T cells). Isotype control stainings are shown by *open histograms*. Numbers in histograms represent averages ± SD of percentages of positive cells ($n = 3$ mice/group). $^*p < 0.0001$ vs. mock in NK populations. $^{**}p < 0.05$ vs. mock in each population

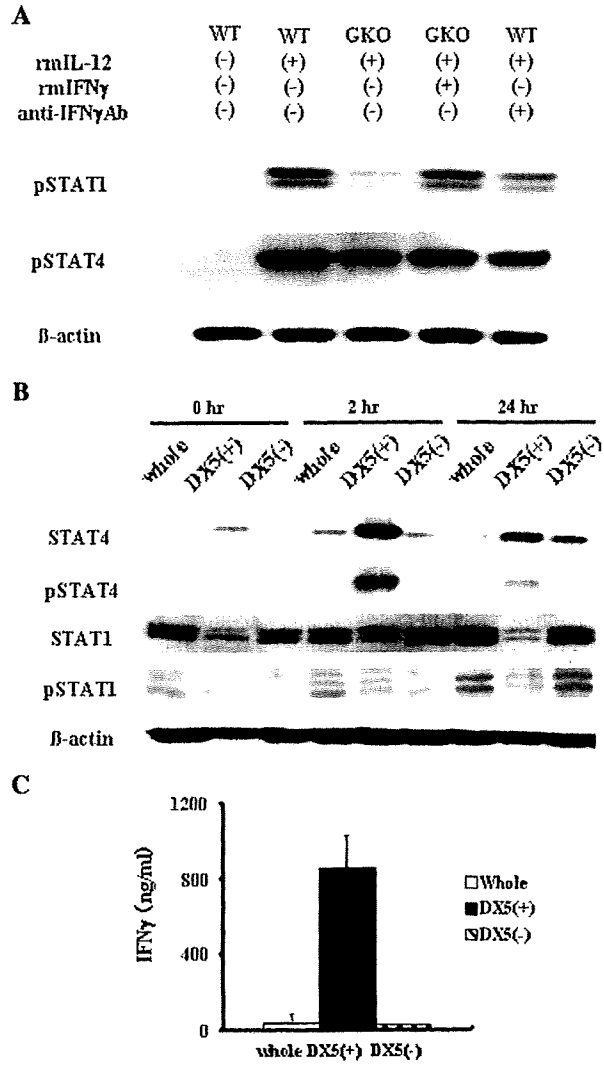


**Fig. 3** STAT signaling and IFNγ production of mononuclear cells in vitro treated with IL-12. **a** STAT1 and STAT4 activation of splenocytes in vitro treated with IL-12. Splenocytes were isolated from wild-type mice or GKO mice and treated with or without recombinant IL-12 (20 ng/mL) in the presence or absence of recombinant IFNγ (500 ng/mL) or anti- IFNγ antibody (20 μg/mL) for 24 h. Cellular lysates were analyzed by Western blot for the expression of phospho-STAT1, phospho-STAT4 and β-actin. **b** and **c** STATs expression and signaling of NK cells and non-NK cells. Splenocytes were isolated from wild-type mice. Whole splenocytes were further purified into $DX5^+$ cells and $DX5^-$ cells. Each cell population was cultured with recombinant IL-12 (20 ng/mL) for the indicated times. **b** The cells were lysed to examine expression of whole STAT and phospho-STAT by Western blot. **c** The levels of IFNγ in the culture supernatant at 24 h were determined by ELISA. Data are expressed as mean and SD ($n = 3$)

cells are sufficient for the anti-metastatic effects of IL-12, we examined the anti-metastatic effect in Rag2 KO mice which lack T cells, B cells and NKT cells. pCMV-IL-12 injection enhanced the Yac1 lytic ability of hepatic mononuclear cells in Rag2 KO mice higher than in wild-type mice (Fig. 4a). To examine whether NK cells are sufficient for IL-12-mediated rejection of hepatic metastasis, we injected pCMV-IL-12 or pCMV into mice that had been intra-splenically injected with CT-26 cells 2 days earlier. Serum IFNγ levels of Rag2 KO mice were about 4 times higher than those of wild-type mice (Fig. 4b). pCMV-IL-12 completely suppressed hepatic metastasis in Rag2 KO mice (Fig. 4c).

## Adoptive transfer of wild-type NK cells into GKO mice restored the anti-tumor effects of IL-12

Since NK cells were sufficient for producing IL-12-induced anti-tumor effects, we postulated that their production of IFNγ may play an important role in these effects. To test this, we performed adoptive transfer experiments with GKO mice. First, whole mononuclear cells isolated from the spleens of wild-type mice ($2.0 \times 10^8$ cells) were adoptively transferred to GKO mice 1 day before plasmid injection. pCMV-IL-12 injection increased Yac1 lytic activity of hepatic mononuclear cells in the adoptively transferred group, but not in the untreated group (Fig. 5a). pCMV-IL-12 induced significant increase in serum IFNγ levels 4 days after plasmid injection in the adoptive transferred group, but not in the other groups (Fig. 5b). The

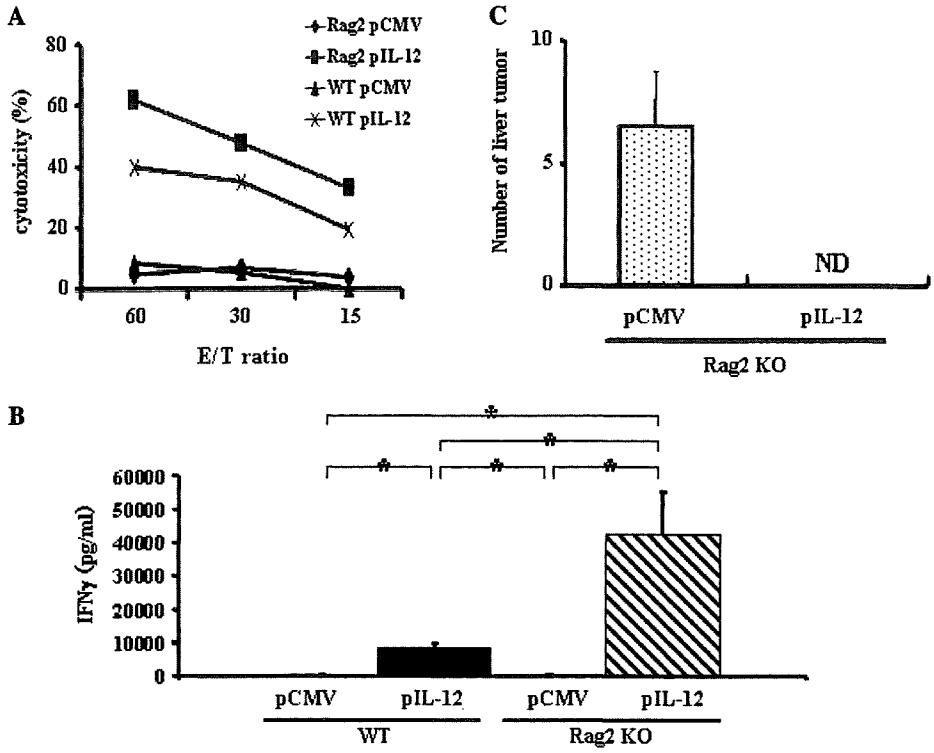


**Fig. 4** Anti-tumor effects of IL-12 in Rag2 KO mice. Serum IFNγ levels and NK-cell activation. Wild-type or Rag2 KO mice were hydrodynamically injected with either pCMV-IL-12 or pCMV and killed at 4 days. **a** Yac1 lytic ability of hepatic mononuclear cells was determined by Cr releasing assay as the indicated effector and target ratios (E/T ratio). Experiments were done 2 times and representative data are shown. **b** The levels of serum IFNγ were determined by ELISA. Data are expressed as mean and SD ($n = 7$/group). *$p < 0.0001$. **c** Anti-metastatic effect. Rag2 KO mice were intrasplenically injected with CT-26 cells and, 2 days later, hydrodynamically injected with either pCMV-IL-12 or pCMV. Fourteen days after plasmid injection, mice were killed to examine tumor development in the liver. The numbers of hepatic tumors in each group are expressed as mean and SD ($n = 7$/group). *ND* not detectable

anti-metastatic effect of IL-12 was restored in GKO mice when whole mononuclear cells from wild-type mice were adoptively transferred (Fig. 5c).

To evaluate the contribution of IFNγ production from each subset of mononuclear cells to the anti-metastatic effect of IL-12, we adoptively transferred the same number of whole mononuclear cells, NK cells or non-NK cells from wild-type mice ($4.0 \times 10^6$ cells) 1 day before pCMV-IL-12 injection and analyzed liver tumor formation. Only in the NK-cell-transferred group, pCMV-IL-12 injection induced NK cytolytic ability in the liver and IFNγ elevation in serum 4 days after plasmid injection, but not in the other groups (Fig. 5d, e). No liver tumor formed in the NK-cell-transferred group. In contrast, livers in other groups had massive tumors, and the liver weights were significantly heavier than those in the NK-cell-transferred group (Fig. 5f). These results clearly demonstrated the strong impact of IFNγ produced from NK cells on IL-12-induced anti-tumor effects compared with that from non-NK cells.

## Anti-tumor effects of IL-12 deteriorated slightly in mice depleted of NK cells

To examine the involvement of NK cells in the tumor deletion by IL-12 therapy, we induced depletion of NK cells by repeatedly injecting anti-asialoGM1 antibody. The cytolytic ability of NK cells was completely abolished in the anti-asialoGM1 antibody-injected group (Fig. 6a). Serum IFNγ induction by IL-12 in the NK depletion group was about half of that in the control immunoglobulin injected group (Fig. 6b). Unexpectedly, pCMV-IL-12 injection inhibited macroscopic liver metastasis of CT-26 cells in NK cell-depleted mice (Fig. 6c). However, a number of microscopic tumor regions were observed after IL-12 therapy in NK cell-depleted mice but not in control IgG-injected mice (Fig. 6d). This finding indicated that NK cells are required for a full-blown IL-12 anti-tumor effect, but IL-12's anti-tumor effect was still observed even if the NK cells were knocked down. To examine the underlying mechanisms of anti-tumor effect in NK cell-depleted mice,

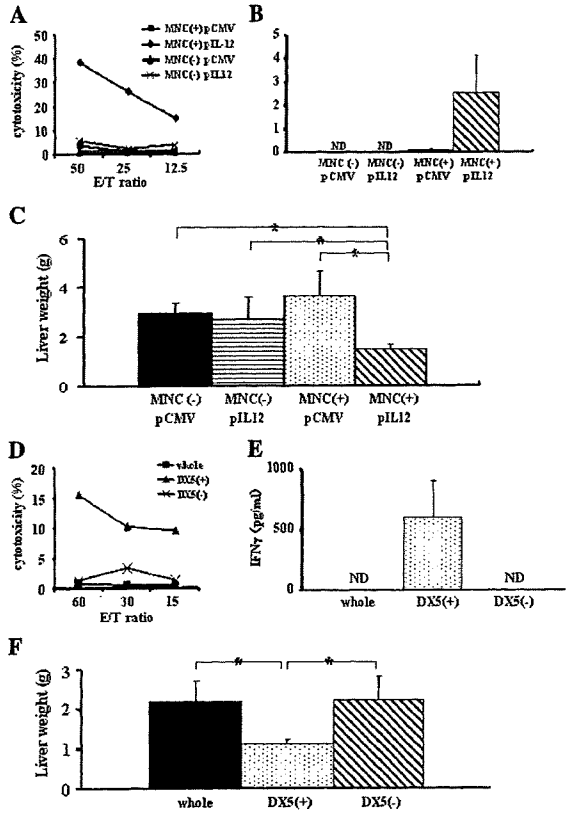


**Fig. 5** Adoptive transfer of wild-type cells into GKO mice. Adoptive transfer of wild-type splenocytes restored anti-tumor effects of IL-12 in GKO mice. **a** GKO mice were intravenously injected with or without $2.0 \times 10^8$ splenocytes from wild-type mice and, 1 day later, hydrodynamically injected with either pCMV-IL-12 or pCMV. Mice were killed 4 days after plasmid injection. Yac1 lytic ability of hepatic mononuclear cells was expressed as the indicated effector and target ratios (E/T ratio). Experiments were done 3 times and representative data are shown. **b** and **c** GKO mice were intrasplenically injected with CT-26 cells and, 1 day later, intravenously injected with or without $2.0 \times 10^8$ splenocytes from wild-type mice. Two days after CT-26 injection, mice were hydrodynamically injected with either pCMV-IL-12 or pCMV. **b** The levels of serum IFNγ 4 days after plasmid injection are expressed as mean and SD ($n$ = 6/group). **c** Fourteen days after plasmid injection, mice were killed to examine liver tumor development by measuring liver weight. The results are indicated as mean and SD ($n$ = 6/group). *ND* not detectable. *$p < 0.01$. Adoptive transfer of wild-type NK cells, but not non-NK cells, restored anti-tumor effects of IL-12 in GKO mice. **d** Wild-type splenocytes were purified into $DX5^+$ cells and $DX5^-$ cells. GKO mice were intravenously injected with $4.0 \times 10^6$ whole mononuclear cells or $DX5^+$ cells or $DX5^-$ cells and, 1 day later, hydrodynamically injected with either pCMV-IL-12 or pCMV. Mice were killed 4 days after hydrodynamic injection. Yac1 lytic ability of hepatic mononuclear cells is expressed as the indicated effector and target ratios (E/T ratio). Experiments were done 3 times and representative data are shown. **e** and **f** GKO mice were intrasplenically injected with CT-26 cells and, 1 day later, intravenously injected with whole mononuclear cells, $DX5^+$ cells or $DX5^-$ cells ($4.0 \times 10^6$/mouse). Two days after CT-26 injection, mice were hydrodynamically injected with either pCMV-IL-12 or pCMV. **e** The levels of serum IFNγ are expressed as mean and SD ($n$ = 6/group). **f** Fourteen days after plasmid injection, mice were killed to examine liver tumor development by measuring liver weight. The results are expressed as mean and SD ($n$ = 6/group). *ND* not detectable. *$p < 0.001$

serum levels of IP-10 and MIG, chemokines downstream of IFNγ, were measured after IL-12 therapy (Fig. 6e). pCMV-IL-12-injected mice showed significant increase in both levels compared with pCMV-injected mice. Significant increase after pCMV-IL-12 injection was also found in NK cell-depleted mice, but not in GKO mice. This result suggests that production of these chemokines was not completely suppressed in NK cell-depleted mice in our experimental condition. Immunohistochemical analysis revealed that tumoral accumulation of CD4-positive cells and CD8-positive cells was observed in pCMV-IL-12-injected mice but not in pCMV-injected mice. On the other hand, similar levels of CD31 expression were observed in tumors of pCMV-injected mice and pCMV-IL-12-injected mice (Fig. 6d). These results suggest that IL-12's anti-tumor effects might be mediated by T-cell accumulating in the tumor rather than anti-angiogenesis.

## Discussion

IL-12 is recognized as a master regulator of adaptive type 1, cell-mediated immunity. One major action of IL-12 is its induction of other cytokines, particularly IFNγ. A large amount of evidence has indicated that IL-12 administration leads to IFNγ production from a variety of immune cells, such as T cells [16], B cells [17], NK cells [18] and NKT cells [22]. The relative impact of each immune cell as the source of IFNγ has been controversial. The present study highlighted NK cells as a most efficient producer of IFNγ that is critical for IL-12-induced anti-tumor effects.

Flow cytometric analysis revealed higher in vivo production of IFNγ of NK cells than that of other cell types. The levels of serum IFNγ were around fourfold higher in Rag2 KO mice which only possess NK cells than in wild-type mice. On the other hand, NK-cell depletion in wild-type mice led to twofold reduction of serum IFNγ levels. These data indicate substantial contribution of NK cells in IFNγ production in vivo. Previous research has demonstrated that the specific cellular effects of IL-12 are due mainly to activation of STAT4 [23, 24]. IL-12-induced STAT4 phosphorylation leads to the production of IFNγ [25]. In agreement with these reports, our in vitro analysis showed that, in contrast to STAT1, STAT4 was directly phosphorylated upon IL-12 stimulation, being independent of IFNγ. Of interest is the finding that NK cells express higher levels of STAT4 than non-NK cells, suggesting that NK cells possess an ideal expression profile of STATs for producing IFNγ upon IL-12 stimulation. Indeed, in vitro analysis revealed that NK cells, upon IL-12 exposure, displayed higher levels of IFNγ production as well as STAT4 phosphorylation than non-NK cells. These in vitro

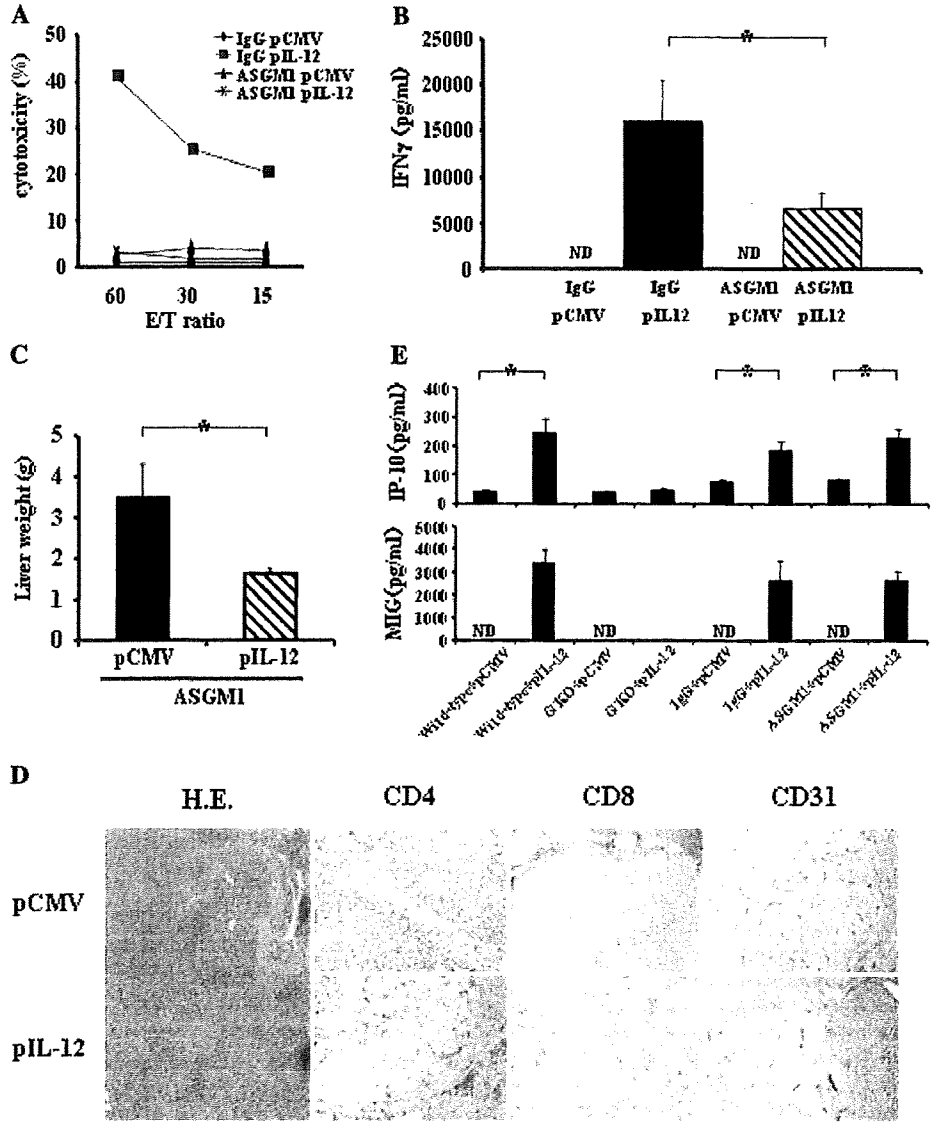


**Fig. 6** Anti-tumor effects of IL-12 in NK-cell-depleted mice. Serum IFNγ levels and NK-cell activation. Wild-type mice were intraperitoneally injected with either anti-asialoGM1 antibody (ASGM1) or control IgG, and, 1 day later hydrodynamically injected with either pCMV-IL-12 or pCMV. Mice were killed 4 days after plasmid injection. **a** Yac1 lytic ability of hepatic mononuclear cells is expressed as the indicated effector and target ratios (E/T ratio). Experiments were done 2 times and representative data are shown. **b** The levels of serum IFNγ are expressed as mean and SD ($n = 6$/group). *ND* not detectable. *$p < 0.005$. Anti-metastatic effects. Wild-type mice were intrasplenically injected with CT-26 cells and, 1 day later and then every 5 days, intraperitoneally injected with either anti-asialoGM1 antibody (ASGM1) or control IgG, and hydrodynamically injected with either pCMV-IL-12 or pCMV 2 days after CT-26 injection. Fourteen days after plasmid injection, mice were killed to examine liver tumor development by measuring liver weight. **c** The results are indicated as mean and SD ($n = 6$/group). *$p < 0.001$. **d** Representative histology of liver sections analyzed by hematoxylin-eosin staining and immunohistochemistry of CD4, CD8 and CD31. **e** Serum levels of IP-10 and MIG. Wild-type or GKO mice were hydrodynamically injected with either pCMV-IL-12 or pCMV. Wild-type mice were intraperitoneally injected with either anti-asialoGM1 antibody (ASGM1) or control IgG, and 1 day later hydrodynamically injected with either pCMV-IL-12 or pCMV. Four days later, each mice were bled to measure the levels of serum IP-10 and MIG. Results are expressed as mean and SD ($n = 6$/group). *ND* not detectable. *$p < 0.001$

data are consistent with the in vivo observation that NK cells are efficient producers of IFNγ during IL-12 therapy.

Many studies have demonstrated that IFNγ production is required for the anti-tumor effects of IL-12 [14, 26, 27]. In fact, we have demonstrated that deletion of IFNγ abolished NK cytotoxicity and the anti-metastatic effect of IL-12 therapy in the liver. A large amount of evidence supports the concept that a major action of IL-12 is to promote the differentiation of naïve CD4 + T cells into Th1 cells, which produce IFNγ. Previous research reported that CD4

T-cell depletion caused inhibition of anti-tumor effects. More recent studies have supported a critical role of IFNγ as a third signal for CD8 T-cell differentiation. There have been many reports focusing on IFNγ production from T cells induced by IL-12 for the anti-tumor effect of IL-12 [28]. Segal et al. performed an elegant study showing a critical role of T-cell production of IFNγ in the anti-tumor effect by adoptively transferring T cells into GKO mice in a subcutaneous tumor model [29]. However, apart from this study, little is known about the contribution of each immune cell as a producer of IFNγ in terms of an anti-tumor effect. In our model, T-cell mediated adaptive responses were not required for the anti-metastatic effect of IL-12. More importantly, the anti-metastatic effects of IL-12 were restored in GKO mice by an adoptive transfer of wild-type NK cells. The same number of non-NK cells could not provoke IL-12-induced anti-tumor effects in GKO mice. The present study demonstrated for the first time a potent effect of NK cells on producing IFNγ that was critical for anti-metastatic effect during IL-12 therapy.

Our study showed that the main IFNγ producer of IL-12 was NK cells. So we focused on NK cells which were activated by IL-12 in an IFNγ-dependent manner to examine the cellular mechanism of protection against hepatic metastasis. Many studies have shown the importance of each subset (NK- [12], NKT- [10] and T [9, 30] cells) for anti-tumor effects of IL-12. In the present study, NK cells were sufficient while T cells, B cells, NKT cells were dispensable for IL-12-mediated NK-cell activation and anti-metastatic effects as IL-12 therapy showed Yac1 lytic ability and antimetastatic effects in Rag2 KO mice. On the other hand, NK-cell depletion by a repeated injection of anti-aialoGM1 antibody protected wild-type mice from macroscopic liver metastasis, but did not from microscopic liver metastasis. Thus, although NK cells were required for a full-blown IL-12 anti-tumor effect, other anti-tumor pathways are activated by IL-12 in the absence of NK cells. Serum levels of IP-10 and MIG suggest that production of these chemokines downstream of IFNγ was not suppressed in NK-cell-depleted mice in our experimental condition. When compared with the experiment on GKO mice, accumulation of CD4-positive cells and CD8-positive cells were more evident in NK-cell-depleted mice than in GKO mice (Supplementary Figure). On the other hand, there was no remarkable difference in the expression of CD31 between pCMV injection and pCMV-IL-12 injection. These results suggested that in NK-cell-depleted mice IL-12 may exert anti-tumor effect via T-cell accumulation rather than anti-angiogenesis.

Since the liver contains an abundance of immune cells (especially NK cells) [31], the cytokine-mediated activation of these cells may be a promising approach toward anti-tumor therapy in this organ [32]. IL-12 is a cytokine known to elicit a potent anti-tumor effect in mouse experimental models. However, clinical trials attempted to date were interrupted by fatal adverse effects. Systemic IL-12 therapy has been associated with dose-limiting toxicity [33]. IL-12 induces activation of the pro-inflammatory pathway which causes the complications of high dose cytokine, independent of the action of IFNγ [34]. On the other hand, the levels of immunosuppressive cytokine, for example, TGF-β1 or IL-10 were significantly higher in patients with hepatocellular cancer and colon cancer [35–38]. In particular, TGF-β1 in serum can limit NK-cell IFNγ production [39]. Thus, in patients with advanced disease, IL-12 may not be able to exert its potent anti-tumor immune-effects because IFNγ, which is an important mediator of the IL-12-induced immune response, is less effective in a tumor environment. In the present study, we demonstrated that NK-cell IFNγ production induced by IL-12 was sufficient for the anti-metastatic effect of IL-12 in the liver. Thus, a strategy of efficiently producing IFNγ from NK cells may be important for avoiding toxicity of IL-12 therapy.

IL-12 gene therapy has an advantage to allow local production of the cytokine at the tumor sites with low serum concentration. Studies demonstrated that intratumoral administration of adenovirus encoding IL-12 to animals with different types of carcinoma caused complete tumor eradication and increased long-term survival [40, 41]. Moreover, injection of IL-12-encoding adenovirus in one nodule of liver tumor resulted in regression of distant nodules in the liver [41]. However, in a clinical trial anti-tumor activity of IL-12-encoding adenovirus was only observed in the injected tumor sites, but not in distant tumors [42]. The present study shed light on hydrodynamic transfection of hepatocytes as a promising strategy to eradicate disseminated tumors from whole liver.

In summary, NK cells are not just an effector for innate immunity but a mediator producing IFNγ that is critical for the IL-12 anti-tumor effects. Extremely higher expression of STAT4 may be a basis for efficient production of IFNγ from NK cells.

**Acknowledgments** We thank Dr. Morihiro Watanabe (Laboratory of Experimental Immunology, Division of Basic Sciences, National Cancer Institute-Frederick Cancer Research and Development Center) for providing the pCMV-IL-12 plasmid, Dr. Yoichiro Iwakura (University of Tokyo, Institute of Medical Science) for providing GKO mice.

## References

1. Kobayashi M, Fitz L, Ryan M, Hewick RM, Clark SC, Chan S, Loudon R, Sherman F, Perussia B, Trinchieri G (1989) Identification and purification of natural killer cell stimulatory factor

(NKSF), a cytokine with multiple biologic effects on human lymphocytes. J Exp Med 170(3):827–845
2. Stern AS, Podlaski FJ, Hulmes JD, Pan YC, Quinn PM, Wolitzky AG, Familletti PC, Stremlo DL, Truitt T, Chizzonite R, Gately MK (1990) Purification to homogeneity and partial characterization of cytotoxic lymphocyte maturation factor from human B-lymphoblastoid cells. Proc Natl Acad Sci USA 87(17):6808–6812
3. Watford WT, Moriguchi M, Morinobu A, O'Shea JJ (2003) The biology of IL-12: coordinating innate and adaptive immune responses. Cytokine Growth Factor Rev 14(5):361–368
4. Trinchieri G (2003) Interleukin-12 and the regulation of innate resistance and adaptive immunity. Nat Rev Immunol 3(2):133–146
5. Colombo MP, Trinchieri G (2002) Interleukin-12 in anti-tumor immunity and immunotherapy. Cytokine Growth Factor Rev 13(2):155–168
6. Del Vecchio M, Bajetta E, Canova S, Lotze MT, Wesa A, Parmiani G, Anichini A (2007) Interleukin-12: biological properties and clinical application. Clin Cancer Res 13(16):4677–4685
7. Wigginton JM, Gruys E, Geiselhart L, Subleski J, Komschlies KL, Park JW, Wiltrout TA, Nagashima K, Back TC, Wiltrout RH (2001) IFN-gamma and Fas/FasL are required for the antitumor and antiangiogenic effects of IL-12/pulse IL-2 therapy. J Clin Invest 108(1):51–62
8. Lee JC, Kim DC, Gee MS, Saunders HM, Sehgal CM, Feldman MD, Ross SR, Lee WM (2002) Interleukin-12 inhibits angiogenesis and growth of transplanted but not in situ mouse mammary tumor virus-induced mammary carcinomas. Cancer Res 62(3):747–755
9. Brunda MJ, Luistro L, Warrier RR, Wright RB, Hubbard BR, Murphy M, Wolf SF, Gately MK (1993) Antitumor and antimetastatic activity of interleukin 12 against murine tumors. J Exp Med 178(4):1223–1230
10. Cui J, Shin T, Kawano T, Sato H, Kondo E, Toura I, Kaneko Y, Koseki H, Kanno M, Taniguchi M (1997) Requirement for Valpha14 NKT cells in IL-12-mediated rejection of tumors. Science 278(5343):1623–1626
11. Zilocchi C, Stoppacciaro A, Chiodoni C, Parenza M, Terrazzini N, Colombo MP (1998) Interferon gamma-independent rejection of interleukin 12-transduced carcinoma cells requires CD4 + T cells and Granulocyte/Macrophage colony-stimulating factor. J Exp Med 188(1):133–143
12. Kodama T, Takeda K, Shimozato O, Hayakawa Y, Atsuta M, Kobayashi K, Ito M, Yagita H, Okumura K (1999) Perforin-dependent NK cell cytotoxicity is sufficient for anti-metastatic effect of IL-12. Eur J Immunol 29(4):1390–1396
13. Takeda K, Hayakawa Y, Atsuta M, Hong S, Van Kaer L, Kobayashi K, Ito M, Yagita H, Okumura K (2000) Relative contribution of NK and NKT cells to the anti-metastatic activities of IL-12. Int Immunol 12(6):909–914
14. Ogawa M, Yu WG, Umehara K, Iwasaki M, Wijesuriya R, Tsujimura T, Kubo T, Fujiwara H, Hamaoka T (1998) Multiple roles of interferon-gamma in the mediation of interleukin 12-induced tumor regression. Cancer Res 58(11):2426–2432
15. Subleski JJ, Hall VL, Back TC, Ortaldo JR, Wiltrout RH (2006) Enhanced antitumor response by divergent modulation of natural killer and natural killer T cells in the liver. Cancer Res 66(22):11005–11012
16. Kubin M, Kamoun M, Trinchieri G (1994) Interleukin 12 synergizes with B7/CD28 interaction in inducing efficient proliferation and cytokine production of human T cells. J Exp Med 180(1):211–222
17. Yoshimoto T, Okamura H, Tagawa YI, Iwakura Y, Nakanishi K (1997) Interleukin 18 together with interleukin 12 inhibits IgE production by induction of interferon-gamma production from activated B cells. Proc Natl Acad Sci USA 94(8):3948–3953
18. Lauwerys BR, Renauld JC, Houssiau FA (1999) Synergistic proliferation and activation of natural killer cells by interleukin 12 and interleukin 18. Cytokine 11(11):822–830
19. Takehara T, Uemura A, Tatsumi T, Suzuki T, Kimura R, Shiotani A, Ohkawa K, Kanto T, Hiramatsu N, Hayashi N (2007) Natural killer cell-mediated ablation of metastatic liver tumors by hydrodynamic injection of IFNalpha gene to mice. Int J Cancer 120(6):1252–1260
20. Watanabe M, Fenton RG, Wigginton JM, McCormick KL, Volker KM, Fogler WE, Roessler PG, Wiltrout RH (1999) Intradermal delivery of IL-12 naked DNA induces systemic NK cell activation and Th1 response in vivo that is independent of endogenous IL-12 production. J Immunol 163(4):1943–1950
21. Takehara T, Suzuki T, Ohkawa K, Hosui A, Jinushi M, Miyagi T, Tatsumi T, Kanazawa Y, Hayashi N (2006) Viral covalently closed circular DNA in a non-transgenic mouse model for chronic hepatitis B virus replication. J Hepatol 44(2):267–274
22. Shin T, Nakayama T, Akutsu Y, Motohashi S, Shibata Y, Harada M, Kamada N, Shimizu C, Shimizu E, Saito T, Ochiai T, Taniguchi M (2001) Inhibition of tumor metastasis by adoptive transfer of IL-12-activated Valpha14 NKT cells. Int J Cancer 91(4):523–528
23. Thierfelder WE, van Deursen JM, Yamamoto K, Tripp RA, Sarawar SR, Carson RT, Sangster MY, Vignali DA, Doherty PC, Grosveld GC, Ihle JN (1996) Requirement for Stat4 in interleukin-12-mediated responses of natural killer and T cells. Nature 382(6587):171–174
24. Kaplan MH, Sun YL, Hoey T, Grusby MJ (1996) Impaired IL-12 responses and enhanced development of Th2 cells in Stat4-deficient mice. Nature 382(6587):174–177
25. Morinobu A, Gadina M, Strober W, Visconti R, Fornace A, Montagna C, Feldman GM, Nishikomori R, O'Shea JJ (2002) STAT4 serine phosphorylation is critical for IL-12-induced IFN-gamma production but not for cell proliferation. Proc Natl Acad Sci USA 99(19):12281–12286
26. Comes A, Di Carlo E, Musiani P, Rosso O, Meazza R, Chiodoni C, Colombo MP, Ferrini S (2002) IFN-gamma-independent synergistic effects of IL-12 and IL-15 induce anti-tumor immune responses in syngeneic mice. Eur J Immunol 32(7):1914–1923
27. Hafner M, Falk W, Echtenacher B, Mannel DN (1999) Interleukin-12 activates NK cells for IFN-gamma-dependent and NKT cells for IFN-gamma-independent antimetastatic activity. Eur Cytokine Netw 10(4):541–548
28. Komita H, Homma S, Saotome H, Zeniya M, Ohno T, Toda G (2006) Interferon-gamma produced by interleukin-12-activated tumor infiltrating CD8 + T cells directly induces apoptosis of mouse hepatocellular carcinoma. J Hepatol 45(5):662–672
29. Segal JG, Lee NC, Tsung YL, Norton JA, Tsung K (2002) The role of IFN-gamma in rejection of established tumors by IL-12: source of production and target. Cancer Res 62(16):4696–4703
30. Nastala CL, Edington HD, McKinney TG, Tahara H, Nalesnik MA, Brunda MJ, Gately MK, Wolf SF, Schreiber RD, Storkus WJ, Lotze MT (1994) Recombinant IL-12 administration induces tumor regression in association with IFN-gamma production. J Immunol 153(4):1697–1706
31. Doherty DG, O'Farrelly C (2000) Innate and adaptive lymphoid cells in the human liver. Immunol Rev 174:5–20
32. Seki S, Habu Y, Kawamura T, Takeda K, Dobashi H, Ohkawa T, Hiraide H (2000) The liver as a crucial organ in the first line of host defense: the roles of Kupffer cells, natural killer (NK) cells and NK1.1 Ag + T cells in T helper 1 immune responses. Immunol Rev 174:35–46
33. Car BD, Eng VM, Lipman JM, Anderson TD (1999) The toxicology of interleukin-12: a review. Toxicol Pathol 27(1):58–63
34. Biber JL, Jabbour S, Parihar R, Dierksheide J, Hu Y, Baumann H, Bouchard P, Caligiuri MA, Carson W (2002) Administration of

two macrophage-derived interferon-gamma-inducing factors (IL-12 and IL-15) induces a lethal systemic inflammatory response in mice that is dependent on natural killer cells but does not require interferon-gamma. Cell Immunol 216(1–2):31–42
35. Tsushima H, Ito N, Tamura S, Matsuda Y, Inada M, Yabuuchi I, Imai Y, Nagashima R, Misawa H, Takeda H, Matsuzawa Y, Kawata S (2001) Circulating transforming growth factor beta 1 as a predictor of liver metastasis after resection in colorectal cancer. Clin Cancer Res 7(5):1258–1262
36. Okumoto K, Hattori E, Tamura K, Kiso S, Watanabe H, Saito K, Saito T, Togashi H, Kawata S (2004) Possible contribution of circulating transforming growth factor-beta1 to immunity and prognosis in unresectable hepatocellular carcinoma. Liver Int 24(1):21–28
37. Chau GY, Wu CW, Lui WY, Chang TJ, Kao HL, Wu LH, King KL, Loong CC, Hsia CY, Chi CW (2000) Serum interleukin-10 but not interleukin-6 is related to clinical outcome in patients with resectable hepatocellular carcinoma. Ann Surg 231(4):552–558
38. Galizia G, Lieto E, De Vita F, Romano C, Orditura M, Castellano P, Imperatore V, Infusino S, Catalano G, Pignatelli C (2002) Circulating levels of interleukin-10 and interleukin-6 in gastric and colon cancer patients before and after surgery: relationship with radicality and outcome. J Interferon Cytokine Res 22(4):473–482
39. Meadows SK, Eriksson M, Barber A, Sentman CL (2006) Human NK cell IFN-gamma production is regulated by endogenous TGF-beta. Int Immunopharmacol 6(6):1020–1028
40. Caruso M, Pham-Nguyen K, Kwong YL, Xu B, Kosai KI, Finegold M, Woo SL, Chen SH (1996) Adenovirus-mediated interleukin-12 gene therapy for metastatic colon carcinoma. Proc Natl Acad Sci USA 93(21):11302–11306
41. Barajas M, Mazzolini G, Genove G, Bilbao R, Narvaiza I, Schmitz V, Sangro B, Melero I, Qian C, Prieto J (2001) Gene therapy of orthotopic hepatocellular carcinoma in rats using adenovirus coding for interleukin 12. Hepatology 33(1):52–61
42. Sangro B, Mazzolini G, Ruiz J, Herraiz M, Quiroga J, Herrero I, Benito A, Larrache J, Pueyo J, Subtil JC, Olague C, Sola J et al (2004) Phase I trial of intratumoral injection of an adenovirus encoding interleukin-12 for advanced digestive tumors. J Clin Oncol 22(8):1389–1397

JOURNAL OF VIROLOGY, Oct. 2009, p. 10427–10436 Vol. 83, No. 20
0022-538X/09/$08.00+0 doi:10.1128/JVI.01035-09


# Cochaperone Activity of Human Butyrate-Induced Transcript 1 Facilitates Hepatitis C Virus Replication through an Hsp90-Dependent Pathway▽

Shuhei Taguwa,[1] Hiroto Kambara,[1] Hiroko Omori,[2] Hideki Tani,[1] Takayuki Abe,[1] Yoshio Mori,[1] Tetsuro Suzuki,[3] Tamotsu Yoshimori,[2] Kohji Moriishi,[1] and Yoshiharu Matsuura[1]*

*Department of Molecular Virology[1] and Department of Cellular Regulation,[2] Research Institute for Microbial Diseases, Osaka University, Osaka, and Department of Virology II, National Institute of Infectious Diseases, Tokyo,[3] Japan*

Received 21 May 2009/Accepted 27 July 2009

**Hepatitis C virus (HCV) nonstructural protein 5A (NS5A) is a component of the replication complex consisting of several host and viral proteins. We have previously reported that human butyrate-induced transcript 1 (hB-ind1) recruits heat shock protein 90 (Hsp90) and FK506-binding protein 8 (FKBP8) to the replication complex through interaction with NS5A. To gain more insights into the biological functions of hB-ind1 in HCV replication, we assessed the potential cochaperone-like activity of hB-ind1, because it has significant homology with cochaperone p23, which regulates Hsp90 chaperone activity. The chimeric p23 in which the cochaperone domain was replaced with the p23-like domain of hB-ind1 exhibited cochaperone activity comparable to that of the authentic p23, inhibiting the glucocorticoid receptor signaling in an Hsp90-dependent manner. Conversely, the chimeric hB-ind1 in which the p23-like domain was replaced with the cochaperone domain of p23 resulted in the same level of recovery of HCV propagation as seen in the authentic hB-ind1 in cells with knockdown of the endogenous hB-ind1. Immunofluorescence analyses revealed that hB-ind1 was colocalized with NS5A, FKBP8, and double-stranded RNA in the HCV replicon cells. HCV replicon cells exhibited a more potent unfolded-protein response (UPR) than the parental and the cured cells upon treatment with an inhibitor for Hsp90. These results suggest that an Hsp90-dependent chaperone pathway incorporating hB-ind1 is involved in protein folding in the membranous web for the circumvention of the UPR and that it facilitates HCV replication.**

Hepatitis C virus (HCV) is the major causative agent of non-A, non-B hepatitis in humans and infects approximately 170 million people worldwide (64). HCV belongs to the genus *Hepacivirus* of the family *Flaviviridae* and is classified into six major genotypes (39). The virus forms small, round, enveloped particles and possesses a genome consisting of a single positive-stranded RNA with a nucleotide length of 9.6 kb. The viral genome encodes a single precursor polyprotein consisting of approximately 3,000 amino acids, which in turn is posttranslationally processed into 10 viral proteins by host and viral proteases. The structural proteins are cleaved from the N-terminal one-fourth of the polyprotein by the host signal peptidase and signal peptide peptidase (36, 43, 44), resulting in the maturation of capsid protein, two envelope proteins, and viroporin p7. The nonstructural protein 2 (NS2) protease cleaves its own carboxyl terminus, and then NS3 cleaves the appropriate downstream positions to produce NS3, NS4A, NS4B, NS5A, and NS5B (24, 60), which form the replication complex, together with several host proteins (14, 35).

NS5A is a membrane-anchored zinc-binding phosphoprotein that appears to possess diverse functions, including the suppression of host defense and the regulation of virus replication (1, 15, 58), but its biological function remains unclear. Several groups, including ours, have suggested that the molecular chaperone, heat shock protein 90 (Hsp90), and several cochaperones participate in the replication complex of HCV through interaction with NS5A or other NS proteins (45, 56, 65). Hsp90 is the highly conserved and ubiquitously expressed protein that acts as a key regulator for the turnover and the activities of more than 200 signaling proteins, including steroid receptors and cell-signaling kinases (66). The chaperone activity of Hsp90 contributes to the refolding of an unfolded protein in an ATP-dependent manner, and the execution of Hsp90-dependent protein folding requires the formation of a multichaperone complex containing other chaperones (e.g., Hsp70, Hsp104, and Hsp40) and cochaperones (e.g., p23, Hop, and immunophilins) (4, 18, 48). Geldanamycin or its derivatives, which are represented as specific inhibitors of Hsp90, can destabilize and then degrade client proteins (41, 55).

The host chaperone mechanism is involved in the folding of viral polymerase to support viral replication (6, 27). Moreover, host chaperones have been reported to play roles in the assembly of viral particles and the sorting of virus proteins (9, 32, 38). We have previously reported that Hsp90 chaperone activities and chaperone-associated proteins are required for the efficient propagation of HCV (45, 56) and that human butyrate-induced transcript 1 (hB-ind1) is involved in the propagation of HCV through interactions with NS5A and Hsp90 via the coiled-coil domain and the FXXW motif, respectively (56). hB-ind1 was first reported to be a multiple-membrane-spanning protein consisting of 362 amino acids that possesses a significant homology with a cochaperones, p23, that regulates

* Corresponding author. Mailing address: Department of Molecular Virology, Research Institute for Microbial Diseases, Osaka University, 3-1, Yamadaoka, Suita-shi, Osaka 565-0871, Japan. Phone: 81-6-6879-8340. Fax: 81-6-6879-8269. E-mail: matsuura@biken.osaka-u.ac.jp.

▽ Published ahead of print on 5 August 2009.

Hsp90 function by its cochaperone activity (11). However, the roles of hB-ind1 in the life cycle of HCV have not been precisely clarified. In this study, we investigated the role of the Hsp90-related chaperone system, including hB-ind1, in the regulation of the RNA replication and particle production of HCV.

## MATERIALS AND METHODS

**Plasmids.** The plasmids encoding hB-ind1, NS5A, Hsp90, and FK506-binding protein 8 (FKBP8) were prepared by methods described previously (45, 56). The DNA fragments encoding hB-ind1 mutants were prepared by PCR with the introduction of a silent mutation that is resistant to the short hairpin RNA in the hB-ind1 knockdown cells, as described previously (56). The human p23 gene and glucose-regulated protein 78 (GRP78) promoter region (−151 to +22) were amplified by PCR from the total cDNA and genomic DNA of Huh7 cells, respectively. The DNA fragments encoding mutants of hB-ind1 and p23 were prepared by the method of splicing by overlap extension (26) and introduced into pEF FLAGGs pGKpuro (28). The GRP78 promoter region was introduced between the KpnI and HindIII sites of pGL3-basic (Promega, Madison, WI) and designated pGRP78-luc. The reporter plasmid carrying a firefly luciferase gene under the control of the GR promoter (pGR-luc) was purchased from Panomics (Fremont, CA). The internal-control plasmid encoding a *Renilla* luciferase (pRL-TK) was purchased from Promega. The plasmid pFK-$I_{389}$ neo/NS3-3′/NK5.1 (47) was kindly provided by R. Bartenschlager. The plasmids used in this study were confirmed by sequencing them with an ABI Prism 3130 genetic analyzer (Applied Biosystems, Tokyo, Japan).

**Cells and virus infection.** All cell lines were cultured at 37°C under a humidified atmosphere and 5% $CO_2$. The human embryonic kidney 293T and hepatocellular carcinoma Huh7 cell lines were maintained in Dulbecco's modified Eagle's medium (DMEM) (Sigma, St. Louis, MO) supplemented with 100 U/ml penicillin, 100 μg/ml streptomycin, and 10% fetal calf serum (FCS). The human hepatocellular carcinoma cell line Huh7.5.1 was kindly provided by F. Chisari (70) and was maintained in DMEM containing nonessential amino acids, 100 U/ml penicillin, 100 μg/ml streptomycin, and 10% FCS. The Huh9-13 cell line, which is a Huh7 cell line harboring a subgenomic HCV RNA replicon (35), was maintained in DMEM containing 10% FCS, nonessential amino acids, and 1 mg/ml G418 (Nakalai Tesque, Kyoto, Japan). The hB-ind1 knockdown cell line Huh-KD and control cell line Huh-ctrl were described previously (56). Huh-KD cells were transfected with each of the expression plasmids encoding wild-type or mutant hB-ind1 and cultured for 1 week in the presence of 10 μg/ml of puromycin. The remaining cells were used for the experiments described below. The viral RNA of JFH1 was introduced into Huh7.5.1 cells according to the method of Wakita et al. (62) for preparation of the infectious HCV particles in cell culture.

**Antibodies.** The rabbit anti-hB-ind1 antibody was prepared as described previously (56). Mouse monoclonal antibodies to HCV NS5A, influenza virus hemagglutinin (HA) and FLAG tags, and β-actin were purchased from Austral Biologicals (San Ramon, CA), Covance (Richmond, CA), and Sigma, respectively. Mouse anti-protein disulfide isomerase (PDI) immunoglobulin G2a (IgG2a) was from Affinity Bioreagents (Golden, CO). Mouse anti-double-stranded RNA (dsRNA) IgG2a (J1 and K2) antibodies were from Biocenter Ltd. (Szirak, Hungary). Alexa Fluor 488 (AF488)-conjugated anti-mouse IgG1, AF647-conjugated anti-rabbit IgG, and AF594-conjugated anti-mouse IgG2a and IgG2b antibodies were from Invitrogen (San Diego, CA).

**Transfection, immunoblotting, and immunoprecipitation.** Transfection and immunoprecipitation analyses were carried out as described previously (25, 45). Immunoprecipitates boiled in loading buffer were subjected to 12.5% sodium dodecyl sulfate-polyacrylamide gel electrophoresis. The proteins were transferred to polyvinylidene difluoride membranes (Millipore, Bedford, MA) and were reacted with the appropriate antibodies. The immune complexes were visualized with Super Signal West Femto substrate (Pierce, Rockford, IL) and detected by an LAS-3000 image analyzer system (Fujifilm, Tokyo, Japan). The protein bands of GRP78 and β-actin were quantified by Multi Gauge software (Fujifilm), and the values of GRP78 expression were normalized with those of β-actin.

**Quantitative reverse transcriptase PCR.** HCV RNA was estimated by the method described previously (56). Total RNA was prepared from cells by using an RNeasy minikit (Qiagen, Tokyo, Japan). First-strand cDNA was synthesized using an RNA LA PCR in vitro cloning kit (Takara Bio Inc., Shiga, Japan) and random primers. Each cDNA was estimated with Platinum SYBR green qPCR SuperMix UDG (Invitrogen) according to the manufacturer's protocol. Fluorescent signals were analyzed with an ABI Prism 7000 (Applied Biosystems). The internal ribosomal entry site regions of HCV and mRNAs of GAPDH (glyceraldehyde-3-phosphate dehydrogenase), GRP78, and growth arrest- and DNA damage-inducible gene 153 (GADD153) were amplified using the primer pairs 5′-GAGTGTCGTGCAGCCTCCA-3′ and 5′-CACTCGCAAGCACCCTATCA-3′, 5′-GAAGGTGAAGGTCGGAGTC-3′ and 5′-GAAGGTGAAGGTCGGAGTC-3′, 5′-CGCCAAGCGGCTCATC-3′ and 5′-AACCACCTTGAACGGCAAGA-3′, and 5′-AGCTGGAACCTGAGGAGAGA-3′ and 5′-TGGATCAGTCTGGAAAAGCA-3′, respectively. The values of the HCV genome or each mRNA were normalized with those of GAPDH mRNA. Each PCR product was detected as a single band of the correct size on agarose gel electrophoresis (data not shown).

In vitro transcription and RNA transfection. The plasmid pFK-$I_{389}$ neo/NS3-3′/NK5.1 was linearized by treatment with ScaI and then transcribed in vitro using the MEGAscript T7 kit (Applied Biosystems) according to the manufacturer's protocol. The in vitro-transcribed RNA was electroporated into cells at 4 million cells/0.4 ml under conditions of 270 V and 960 μF using a Gene Pulser (Bio-Rad, Hercules, CA). The colony formation assay was carried out by a method described previously (45).

**Indirect immunofluorescence assay.** Cells cultured on glass slides were fixed with 4% paraformaldehyde in phosphate-buffered saline (PBS) at room temperature for 30 min. After being washed twice with PBS, the cells were permeabilized for 20 min at room temperature with PBS containing 0.25% saponin and blocked with PBS containing 0.2% gelatin (gelatin-PBS) for 60 min at room temperature. The cells were incubated with gelatin-PBS containing rabbit anti-hB-ind1 antibody, mouse anti-NS5A IgG1, mouse anti-PDI IgG2a, mouse anti-FKBP8 IgG2b, or mouse anti-dsRNA IgG2a (J1 and K2) at 37°C for 60 min; washed three times with PBS containing 1% Tween 20; and incubated with gelatin-PBS containing AF488-conjugated anti-mouse IgG1 or AF647-conjugated anti-rabbit or AF594-conjugated anti-mouse IgG2a or IgG2b antibodies at 37°C for 60 min. Finally, the cells were washed three times with PBS containing 1% Tween 20 and observed with a FluoView FV1000 laser scanning confocal microscope (Olympus, Tokyo, Japan).

**Correlative FM-EM.** Correlative fluorescence microscopy-electron microscopy (FM-EM) allows individual cells to be examined both in an overview with FM and in a detailed subcellular-structure view with EM (51). The endogenous hB-ind1 and NS5A were stained and observed in the HCV replicon cells by the correlative FM-EM method as described previously (45).

**Luciferase assay.** Each plasmid was transfected into Huh7, Huh9-13, and interferon (IFN)-cured cells seeded in a 12-well plate, and the cells were treated with 1 μM dexamethasone (Sigma) for 12 h or with 17-dimethylamino-ethylamino-17-demethoxygeldanamycin (DMAG) (Sigma) for 6 h at 36 h posttransfection and lysed in 200 μl of passive lysis buffer (Promega). Luciferase activity was measured in 20-μl aliquots of the cell lysates using a Dual-Luciferase Reporter Assay System (Promega). Firefly luciferase activity was standardized with that of *Renilla* luciferase cotransfected with the internal-control plasmid pRL-TK. The resulting values were expressed as the increase in relative light units (RLU).

**Statistical analysis.** Results were expressed as the mean ± standard deviation. The significance of differences in the means was determined by Student's *t* test.

## RESULTS

**The p23-like domain of hB-ind1 has cochaperone activity.** Although we had previously reported that hB-ind1 regulates HCV RNA replication through interaction with NS5A and Hsp90, the molecular mechanisms underlying the regulation of HCV replication remained to be clarified. To gain more insights into the potential cochaperone activity of hB-ind1 in the Hsp90 chaperone system, we prepared expression plasmids encoding a wild-type p23 and three p23 mutants—one in which the FXXW motif was replaced with AXXA (p23AxxA), one in which the cochaperone domain of p23 was replaced with the p23-like domain of hB-ind1 (cp23), and one in which both substitutions were made (cp23AxxA) (Fig. 1A). HA-tagged Hsp90 was coexpressed with FLAG-tagged p23 or the FLAG-tagged p23 mutants in 293T cells (Fig. 1B). Hsp90 was coimmunoprecipitated with wild-type p23 and a cp23 mutant, but not with the p23AxxA or cp23AxxA mutants, indicating that the FXXW motif of hB-ind1, as is the case with that of p23

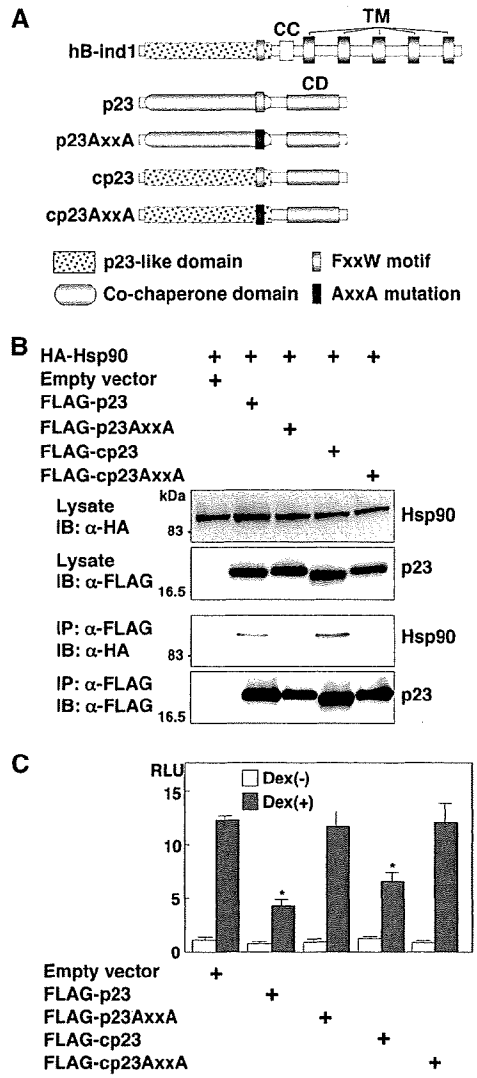


FIG. 1. Construction and characterization of p23 mutants. (A) Structures of hB-ind1, p23, and the three p23 mutants. hB-ind1 consists of a p23-like domain, an FXXW motif, a coiled-coil domain (CC), and a transmembrane domain (TM). p23 consists of a cochaperone domain, an FXXW motif, and a chaperone domain (CD). The three p23 mutants, p23AxxA, cp23, and cp23AxxA, were constructed by replacing the FXXW motif with AXXA, the cochaperone domain of p23 with the p23-like domain of hB-ind1, and both of the regions, respectively. (B) FLAG-tagged p23, p23AxxA, cp23, or cp23AxxA was coexpressed with HA-tagged Hsp90 in 293T cells and immunoprecipitated (IP) with anti-FLAG antibody. The immunoprecipitates were subjected to immunoblotting (IB). (C) The expression plasmid encoding FLAG-tagged p23, cp23, p23AxxA, or cp23AxxA was cotransfected with pGR-luc and pRL-TK plasmids into 293T cells and treated with 1 mM dexamethasone [Dex(+)] at 36 h posttransfection or untreated [Dex(−)], and the luciferase activities were determined at 12 h of incubation. The firefly luciferase activity was normalized with that of *Renilla* luciferase, and the GR-responsive promoter activity was indicated as the RLU. The error bars indicate standard deviations. The asterisks indicate significant differences ($P < 0.01$) versus the control value. The data shown are representative of three independent experiments.

(67), is also involved in binding to Hsp90. Hsp90 participates in the folding and stabilization of the ligand-binding domain of the glucocorticoid receptor (GR), together with p23 and other cofactors (49). p23 was shown to act not only in the activation (30), but also in the inhibition, of GR signaling (67). To examine whether hB-ind1 has the ability to work as a cochaperone in an Hsp90-dependent manner, each of the plasmids encoding p23 or the p23 mutants was cotransfected with a reporter plasmid carrying a firefly luciferase gene under the control of the GR promoter (pGR-luc), together with an internal-control plasmid (pRL-TK), and GR-mediated transcriptional activity was determined at 12 h after treatment with dexamethasone, a ligand of GR. Expression of the p23 or cp23 mutant, but not of the AXXA mutants, significantly inhibited GR-mediated transcription (Fig. 1C). These results indicate that the p23-like domain of hB-ind1 possesses cochaperone activity comparable to that of p23.

**The p23-like domain of hB-ind1 is interchangeable with the p23 cochaperone domain during complex formation with NS5A, Hsp90, and FKBP8.** Previous reports have suggested that HCV NS5A interacts with several host proteins, including FBL2 (63), vesicle-associated membrane protein-associated protein subtype A (VAP-A) (61), VAP-B (25), FKBP8 (45), and hB-ind1 (56), and that these interactions participate in the replication of HCV. We have shown that hB-ind1 interacts with NS5A and Hsp90 through the coiled-coil domain and the FXXW motif in the p23-like domain, respectively, and that coexpression of FKBP8 enhances the interaction of Hsp90 with hB-ind1 (56). To determine the effect of the mutation in the p23-like domain of hB-ind1 on interaction with Hsp90, NS5A, and FKBP8, we prepared an expression plasmid encoding wild-type hB-ind1 and three hB-ind1 mutants, one in which the p23-like domain was replaced with the cochaperone domain of p23 (chB-ind1), one in which the FXXW motif was replaced with AXXA (hB-ind1AxxA), and one in which both replacements were made (chB-ind1AxxA) (Fig. 2A). The FLAG-tagged wild-type or mutant hB-ind1 was coexpressed with HA-tagged Hsp90 (Fig. 2B, left) or HA-tagged NS5A (Fig. 2B, right) in 293T cells and immunoprecipitated with anti-FLAG antibody. Hsp90 was coprecipitated with wild-type hB-ind1 and the chB-ind1 mutant, but not with the hB-ind1AXXA and chB-ind1AXXA mutants (Fig. 2B, left), confirming that the FXXW motif is crucial for the interaction with Hsp90. In contrast, NS5A was coprecipitated with each of the hB-ind1 proteins, suggesting that mutation in the p23-like domain of hB-ind1 has no effect on the binding of hB-ind1 to NS5A through the coiled-coil domain (Fig. 2B, right). To determine the effect of FKBP8 expression on the interaction between hB-ind1 and Hsp90, FLAG-tagged wild-type hB-ind1 or the chB-ind1 mutant was coexpressed with HA-tagged FKBP8 and/or Hsp90 in 293T cells and immunoprecipitated with anti-FLAG antibody. The amounts of Hsp90 coprecipitated with hB-ind1 or chB-ind1 were increased by coexpression of FKBP8 (Fig. 2C). To further examine the interaction of hB-ind1 with Hsp90 and NS5A at an endogenous expression level in Huh9-13 cells harboring an HCV subgenomic RNA replicon, lysates of the replicon cells were subjected to immunoprecipitation analysis. Endogenous Hsp90 and NS5A were specifically coimmunoprecipitated with endogenous hB-ind1 (Fig. 2D). These results suggest that the p23-like domain of hB-ind1 is inter-

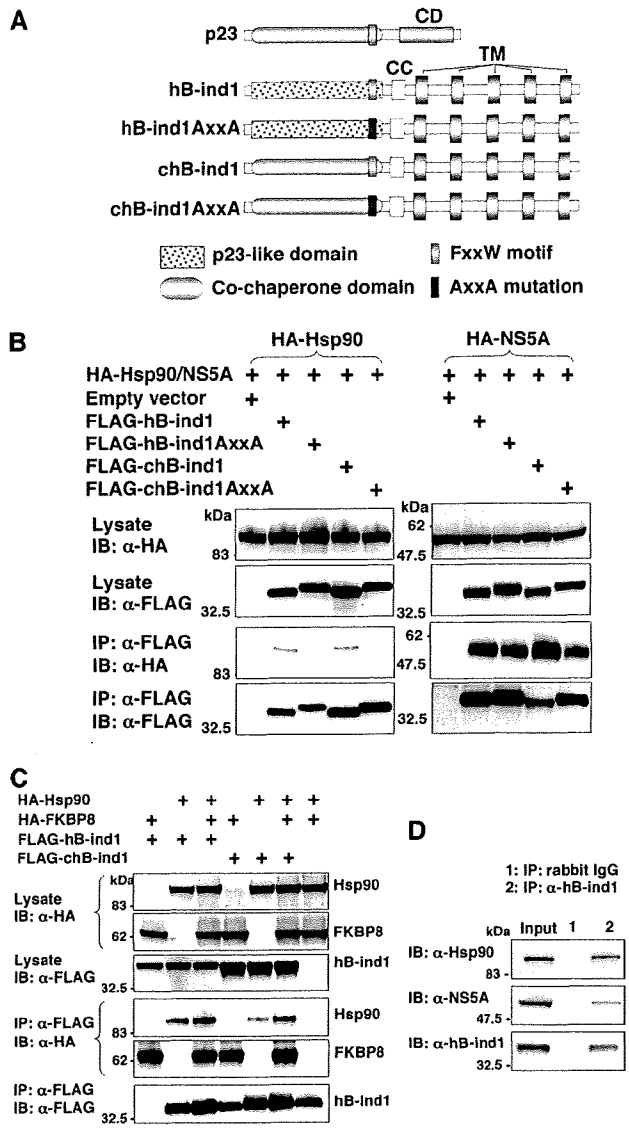


FIG. 2. Construction and characterization of hB-ind1 mutants. (A) Structures of p23, hB-ind1, and the three hB-ind1 mutants. The three hB-ind1 mutants, hB-ind1AxxA, chB-ind1, and chB-ind1AxxA, were constructed by replacing the FXXW motif with AXXA, the p23-like domain of hB-ind1 with the cochaperone domain of p23, and both of the regions, respectively. (B) FLAG-tagged hB-ind1, hB-ind1 AxxA, chB-ind1, or chB-ind1AxxA was coexpressed with either HA-tagged Hsp90 (left) or NS5A (right) in 293T cells and immunoprecipitated (IP) with anti-FLAG antibody. The immunoprecipitates were subjected to immunoblotting (IB). (C) HA-tagged Hsp90 and HA-FKBP8 were expressed with FLAG-tagged hB-ind1 and chB-ind1 in various combinations in 293T cells and immunoprecipitated with anti-FLAG antibody, and the immunoprecipitates were detected by immunoblotting. (D) Endogenous hB-ind1 in Huh9-13 cells harboring subgenomic HCV replicon RNA was immunoprecipitated with anti-hB-ind1 rabbit IgG (lane 2). The cell lysate was mixed with normal rabbit IgG as a negative control (lane 1). The immunoprecipitates were analyzed by immunoblotting with an antibody to Hsp90, NS5A, or hB-ind1. The data shown are representative of three independent experiments.

changeable with the cochaperone domain of p23 during complex formation with NS5A, Hsp90, and FKBP8.

**Cochaperone activity in the p23-like domain of hB-ind1 is required for propagation of HCV.** The p23-like domain of hB-ind1 has been suggested to be required for HCV propagation (56). However, the involvement of the cochaperone activity of hB-ind1 in HCV propagation has not been examined. To assess the effect of cochaperone activity in the p23-like domain of hB-ind1 on the RNA replication and particle production of HCV, each of the expression plasmids encoding the FLAG-tagged wild-type or mutant hB-ind1 carrying the silent mutations resistant to small interfering RNA was transfected into hB-ind1 knockdown (Huh-KD) cells and cultured for a week in the presence of puromycin. The expressions of FLAG-tagged hB-ind1 and the mutants in the Huh-KD cells were comparable to that of the endogenous hB-ind1 in the control (Huh-ctrl) cells transfected with an empty vector (Fig. 3A). Subgenomic HCV replicon RNA transcribed from pFK-$I_{389}$ neo/NS3-3′/NK5.1 was transfected into these cells and cultured for 4 weeks in the presence of G418. Although the number of colonies was reduced in the Huh-KD cells compared with the Huh-ctrl cells after transfection with an empty vector, as described previously (56), the colony numbers were recovered by the expression of the hB-ind1 or chB-ind1 mutant, but not by that of the hB-ind1AXXA or chB-ind1AXXA mutants (Fig. 3B). Similarly, intracellular HCV RNA and infectious viral titers in the culture supernatants of Huh-KD cells infected with JFH1 virus were partially recovered by the expression of the hB-ind1 or chB-ind1 mutant, but not by that of the hB-ind1AXXA or chB-ind1AXXA mutant (Fig. 3C). These results suggest that cochaperone activity in the p23-like domain of hB-ind1 is required for HCV propagation and that the cochaperone domain of p23 can substitute for the p23-like domain of hB-ind1.

**hB-ind1 colocalizes with NS5A, FKBP8, and dsRNA on the membranous web.** Our previous report revealed the interplay among hB-ind1, Hsp90, FKBP8, and NS5A and showed that these interactions play an important role in HCV replication (56). However, the subcellular localization of the endogenous hB-ind1 in the replicon cells and JFH1 virus-infected cells has not been precisely assessed. To determine the subcellular localization of hB-ind1 in the context of HCV replication, the expression of hB-ind1 and NS5A in the replicon cells and JFH1 virus-infected cells was examined by immunofluorescence analyses (Fig. 4A). Endogenous hB-ind1 was colocalized with the endoplasmic reticulum (ER)-marker PDI and NS5A as dot-like structures in the Huh9-13 replicon cells (Fig. 4A, top) and in cells infected with JFH1 virus (Fig. 4A, bottom), and these dot-like structures disappeared in concert with the loss of NS5A expression by treatment with IFN-α in the replicon cells and was not observed in the mock-infected Huh7.5.1 cells. Furthermore, FKBP8 (Fig. 4B, top) and dsRNA (Fig. 4B, bottom) were colocalized with hB-ind1 and NS5A in the dot-like structures in Huh9-13 replicon cells. These results indicate that HCV replicating RNA is localized with hB-ind1, FKBP8, and NS5A in the dot-like compartments. HCV RNA replication or expression of viral proteins leads to formation of the convoluted membranous structures designated the membranous web (14, 23). The large structures of the replication complexes in the replicon cells indicate membranous webs with